5-2024

Green Synthesis Of Silver And Titanium Nanoparticles Using Erythrina Variegata Root Bark Extract And Evaluation Of Their Antioxidant And Cytotoxicity Effectiveness

Naiyah McDaniel

GREEN SYNTHESIS OF SILVER AND TITANIUM NANOPARTICLES USING *ERYTHRINA VARIEGATA* ROOT BARK EXTRACT AND EVALUATION OF THEIR ANTIOXIDANT AND CYTOTOXICITY EFFECTIVENESS

A Thesis

By

Naiyah McDaniel

Submitted to the Office of Graduate Studies of
Prairie View A&M University
in partial fulfillment of the requirements for the degree of

MASTER OF SCIENCE

May 2024

Major Subject: Chemistry

GREEN SYNTHESIS OF SILVER AND TITANIUM NANOPARTICLES USING *ERYTHRINA VARIEGATA* ROOT BARK EXTRACT AND EVALUATION OF ANTIOXIDANT AND CYTOTOXIC EFFECTIVENESS

A Thesis

By

Naiyah McDaniel

Submitted to the Office of Graduate Studies of
Prairie View A&M University
in partial fulfillment of the requirements for the degree of

MASTER OF SCIENCE

Approved as to style and content by:

Harshica Fernando Chair of Committee	Marco Giles Committee Member
Gina Chiarella Committee Member	Ananda Amarasekara Head of Department
Ananda Amarasekara Committee Member	Dorie J. Gilbert Dean of the College of Arts & Sciences

Tyrone Tanner
Dean of Graduate Studies

May 2024

Major Subject: Chemistry

ABSTRACT

Green Synthesis of Silver and Titanium Nanoparticles Using *Erythrina Variegata* Root Bark Extract and Evaluation of Their Antioxidant and Cytotoxic Effectiveness

(May 2024)

Naiyah McDaniel, B.S., Prairie View A&M University

Chair of Advisory Committee: Dr. Harshica Fernando

Erythrina variegata belongs to the *Erythrina* genus, which consists of approximately 110 species of trees and shrubs. In its native regions, different parts of the plant have been used for its effectiveness in treating asthma, epilepsy, bacterial infections, and wounds. Characterization studies have been done for this plant, and researchers have identified several alkaloids, flavonoids, and other active phytoconstituents that help treat different ailments. Prior research has focused on the phytochemical profile of E. *variegata's* leaves, flowers, and stem bark. This work aimed to address gaps in the characterization of *E. variegata's* root bark while exploring the effectiveness of titanium and silver nanoparticles in cytotoxicity, antioxidant, electrochemical studies, and bioactive property enhancement. Overall research questions included whether the phytochemical profile of this medicinal plant could be expanded and whether this plant possessed antioxidant and cytotoxic capabilities to be used in human and environmental health applications. The methodology included preparing *E. variegata* root bark extract, examining bioactive compounds in the pure extract alone via

GC-MS, and using the extract to synthesize silver and titanium nanoparticles. The synthesized nanoparticles were characterized using UV-visible spectroscopy, Fourier Transform Infrared spectroscopy (FTIR), Scanning Electron Microscopy (SEM), Energy Dispersive X-ray spectroscopy (EDS), and dynamic light scattering experiments. The mass spectrometry results confirm the presence of bioactive compounds known to belong to the Erythrina genus and some compounds unique to the root bark. Characterization studies confirmed the formation of titanium and silver nanoparticles using the plant's extract. While examining the radical scavenging and cytotoxicity effectiveness of the plant nanoparticles, it was discovered that silver and titanium nanoparticles synthesized using the root bark extract could maintain and enhance specific bioactive properties of the plant. The research presented in this work sought to enhance current knowledge on chemical components regarding *E. variegata* and examine changes in phytochemical properties when used to synthesize silver and titanium nanoparticles. Through characterization experiments and the conduction of foundational application studies, this study was designed to contribute to the progress of incorporating natural products to enhance human and environmental health while promoting the use of green chemistry techniques.

Index Terms- Erythrina variegata, dynamic light scattering (DLS), energy dispersive X-ray spectroscopy (EDS), fourier transform infrared spectroscopy (FTIR), gas chromatography-mass spectrometry (GC-MS), green nanoparticle synthesis, scanning electron microscopy (SEM), ultra-violet visible spectroscopy (UV).

DEDICATION

I dedicate this thesis to my Lord and Savior, Jesus Christ. To Him be all the honor and glory. Without Him, I am nothing, and none of this would be possible. I am so grateful for His grace and mercy that carried me through this journey. To my sister, I hope this will inspire you and remind you that you can do anything you set your mind to. Lastly, for my family, I dedicate this to you. Without you all, none of this would have been possible. Thank you for your endless support and love through this whole process.

ACKNOWLEDGEMENTS

First, I would like to acknowledge and thank my mentor, Dr. Harshica Fernando. Thank you for constantly pushing me to pursue the best, even when I did not want it for myself. I learned so much while working with you, and I appreciate you always considering me for opportunities. You are the best mentor I could have asked for. Thank you for supporting me through every step of this journey. I also want to thank everyone in the Prairie View A&M Department of Chemistry. I greatly appreciate all the knowledge and support you have given me during my time here. Thank you for always considering me for opportunities and providing me with resources to ensure my success.

TABLE OF CONTENTS

Page

NOMENCLATURE

AgNPs	Silver Nanoparticles
CO_2	Carbon Dioxide
CV	Cyclic Voltammetry
DLS	Dynamic Light Scattering
DPPH	1,1-Diphenyl-2-picrylhydrazyl
EBI	Bowman-Birk family proteinase inhibitor
ECI	Kunitz family inhibitors
EC_{50}	Half-maximal effective concentration
EDS	Energy Dispersive X-ray Spectroscopy
ETIa	Kunitz family inhibitors
EV	Erythrina *variegata*
EvAgNPs	Erythrina *variegata* silver nanoparticles
EvTiNPs	Erythrina *variegata* titanium nanoparticles
FTIR	Fourier Transform Infrared Spectroscopy
GC-MS	Gas Chromatography-Mass Spectroscopy
HPLC	High-Performance Liquid Chromatography
IC_{50}	The concentration of a drug that is required for 50% inhibition
MBC	Minimum Bactericidal Concentration
MIC	Minimum Inhibitory Concentration
mm	Millimeter
mL	Milliliter

MTS	3-(4,5-dimethylthiazol-2-yl)-5-(3-carboxymethoxyphenyl)-2-(4-sulfophenyl)-2H-tetrazolium
NO	Nitric Oxide
NO_2	Nitrogen Dioxide
PBS	Phosphate Buffered Saline
ROS	Reactive Oxygen Species
RNS	Reactive Nitrogen Species
SEM	Scanning Electron Microscopy
SO_2	Sulfur Dioxide
TiNPs	Titanium Nanoparticles
TiO_2	Titanium Dioxide
Tris-HCl	Tris(hydroxymethyl)aminomethane Hydrochloride
µg	Microgram
µL	Microliter

LIST OF FIGURES

FIGURE Page

LIST OF TABLES

1. INTRODUCTION

Plants possess a rich history in their ties to human health. From their use in traditional medicine to their natural function as environmental health regulators, the connection between human health and nature is undeniable. The relationship between humans and plants presents the opportunity to be mutually beneficial. With plants' natural ability to remove toxic substances through chemical cycling and their historical use in treating various ailments, there is abundant opportunity to address pollution affecting environmental health and economic accessibility to health care. While natural products present an avenue to promote human health, many studies still need to be done to characterize the compounds contributing to the medicinal properties of plants. Additionally, due to current levels of human activity, the human population significantly contributes to increased amounts of ecological contaminants, adversely affecting human health and plants' ability to perform their natural function. After providing a brief overview of the historical medicinal use of plants and their role in the environment, this thesis aimed to explore the use of natural products for human and environmental health by examining a traditional medicinal plant, *Erythrina Variegata*, with emphasis on attempting to enhancing its bioactivity when used to synthesize silver and titanium nanoparticles.

This thesis follows the style of the Institute of Electrical and Electronics Engineers

1.1 Historical Use of Medicinal Plants

The earliest records regarding medicinal plant use date back to 2600 BC and highlight methods for performing plant-based therapy for disease treatment in Egyptian, Chinese, Mesopotamian, and Indian societies [1]. Natural products native to different geographic locations have long been utilized by healthcare providers and marketed for consumer use to treat illnesses such as HIV, AIDS, malaria, Alzheimer's, tuberculosis, and blood disorders [2]. The use of natural products for disease treatment remains a popular approach to healthcare needs in many Eastern countries due to widespread accessibility and economic affordability [3]. Additionally, 5.7 and 8.4 million deaths are attributed to poor-quality care each year in low- and middle-income countries, influencing widespread consumer preference for natural products and self-medication [1]. Though the Western front of medicine has diverged from natural product-based roots, opting for creating synthetic compounds similar to those in plants, the global scientific community is seeing a resurgence of consideration for using plant-based disease treatment.

In both geographic areas, there is a need for further exploration regarding plants possessing medicinal properties. The Eastern world maintains a rich history of traditional medicine practices, but medicinal plant use occurred without mechanistic or scientific knowledge of compounds contributing to therapeutic efficiency [1]. In turn, the Western world is suffering from a primary focus on deriving synthetic compounds, causing a decline in drug production and the creation of effective medications [4]. While the movement has begun to identify and characterize secondary metabolites contributing to medicinal plant properties, there is still a drastic need for scientific discovery in the field for both sectors, as only approximately six percent of plant species have been

pharmacologically investigated, and only 15% studied phytochemically [1]. Scientific engagement toward the characterization and identification of the bioactive compounds present in traditionally medicinal plants represents a global solution to improving human health, allowing medical treatment to become more accessible, economically friendly, and capable of treating more diseases.

1.2 Environmental Uses of Plants

Plants possess the capacity to remediate areas of environmental pollution. In addition to their natural ability to remove toxins from the air through photosynthesis and chemical cycling, certain plants can assimilate, degrade, or modify atmospheric pollutants like SO_2, NO_2, and CO_2 into less toxic ones, restoring ecological balance [5]. Phytoremediation is a green chemistry technique that takes advantage of these unique properties in plants and can potentially remediate atmospheric environmental pollutants through plants [6]. This technique represents a low-cost, eco-friendly solution to address growing environmental concerns regarding increasing atmospheric pollution.

Current atmospheric conditions are drastically decreasing due to human activities such as fuel combustion, transportation, and smoking, contributing to the release of vast amounts of nitrogen, sulfur, and carbon oxides. Environmentally, the abundance of these pollutants in the atmosphere accelerates global warming and climate change. As a result, on the molecular level, reactive oxidative species (ROS) are increasing in human cells[7]. In addition to oxidative stress, the impacts of increased environmental pollution cause reduced lung function, inflammation, asthma attacks, and excess respiratory and cardiac hospital admissions [8]. With fossil fuel combustion accounting for the primary energy source for power and transportation coupled with the slowness of renewable energy

sources to gain traction, it is evident that the sources of pollution are not going away anytime soon. There remains a need to examine methods to remedy the damage human activity is causing to the environment and human health. Phytoremediation offers a solution to growing environmental concerns and provides the opportunity to improve human health. Still, to successfully implement this technique, scientists must further investigate the biochemical processes and secondary metabolites affecting the uptake of pollutants. The research presented in this thesis aimed to identify the capability of a specific plant to scavenge free radicals, which contribute to oxidative stress in humans and the formation of certain pollutants in the environment.

1.3 Erythrina variegata

Erythrina variegata is a plant native to India, Malaysia, Zanzibar, and parts of Polynesia [9]. This plant is a coral tree, growing 50 to 60 feet tall, and is most known for its variegated leaves and red flowers. In its native areas, *E. variegata* leaves, flowers, and bark have been used traditionally for analgesic, antiasthmatic, antiseptic, and anti-inflammatory purposes [9]. Additionally, *E. variegata's* alkaloid and flavonoid phytoconstituents have been isolated in studies exploring antibacterial efficacy, cytotoxicity, and effects on the central nervous system. While existing research characterizes several phytoconstituents and secondary metabolites in *E. variegata*, current research heavily focuses on the chemical profile of the plant's leaves and flowers, creating a gap in reporting the chemical constituents in the plant's root bark. This thesis aimed to address the gap in the characterization of *E. variegata's* root bark while exploring the effectiveness of its' root bark extract in cytotoxicity, antioxidant, and electrochemical studies- additionally, conducting experiments testing bioactive property

enhancement of *E. variegata* root bark through silver and titanium nanoparticle synthesis, each of which possesses their own unique bioactive capabilities. The research presented in this thesis sought to enhance the current knowledge base of chemical components regarding traditionally medicinal plants while conducting foundational studies to contribute to the progress of incorporating natural products to improve human and environmental health.

In conclusion, Chapter 1 overviews the history of traditional medicine and presents the benefits natural products can provide for human health. Additionally, this chapter brings awareness to environmental concerns affecting human health, providing information on a green solution to remedy these issues while introducing the plant of discussion for this thesis and connecting it to research goals to expand natural product medicine and reduce environmental pollution. The remainder of this study examines current research conducted with *E. variegata* and theoretical information contributing to methodology development and experimental design in Chapter 2. Chapter 3 provides the details of the methods used in performing each experiment, and, in conclusion, Chapters 4 and 5 discuss the results and conclusions drawn from the research conducted.

‘

2. LITERATURE REVIEW

2.1 Identified Phytoconstituents of E. variegata

E. variegata is predominantly native to tropical Asian regions such as China, Malaysia, Indonesia, Thailand, India, and areas of East Africa. This plant has maintained its traditional ethnomedical use, treating convulsions, inflammation, bacterial infections, hyperglycemia, and asthma in these areas [11], [12]. As worldwide research interests have grown regarding the use of natural products, studies have examined the phytoconstituents that contribute to the effectiveness of these products in treating certain conditions. Regarding the *Erythrina* genus, scientists have identified the presence of alkaloids, flavonoids, pterocarpans, triterpenes, steroids, and proteins in various parts of the plant, resulting in medicinal effectiveness.

Phytochemical studies on *E. variegata* identify alkaloids and flavonoids as the primary phytoconstituents present in the plant. Fig. 1 represents a few phytoconstituents identified using ^{1}H-NMR and ^{13}C-NMR for *Erythrina variegata*. With tetracyclic alkaloids: (+)-3-Demethoxyerythratidinone, (+)-erythraline, (+)-erythramine, (+)-erythrinine, (+)-erythratidinone, (+)-erysonine, (+)-erysotine, (+)-erysodine, (+)-erysovine, (+)-11-hydroxyepierythratidine, (+)-erythratidine, (+)-epierythratidine, (+)-erysodienone, (+)-erysotrine, (+)-erysopitine, (+)-11-β-hydroxyerysotrine[(+)-erythrartine] isolated from different parts of the *E. variegata [12]* and isoflavonoids: erythrinins A, B, and C, osajin and alpinum isoflavone, styrene oxyresveratrol, stigmasterol, erystagallin A, erycricstagallin, orientanol B, erycristgallin, dihydrostilbene

dihydroxyresveratrol [12], [13], [14]. Other phytoconstituents reported included erythrabyssin II and dihydrofolinin [15].

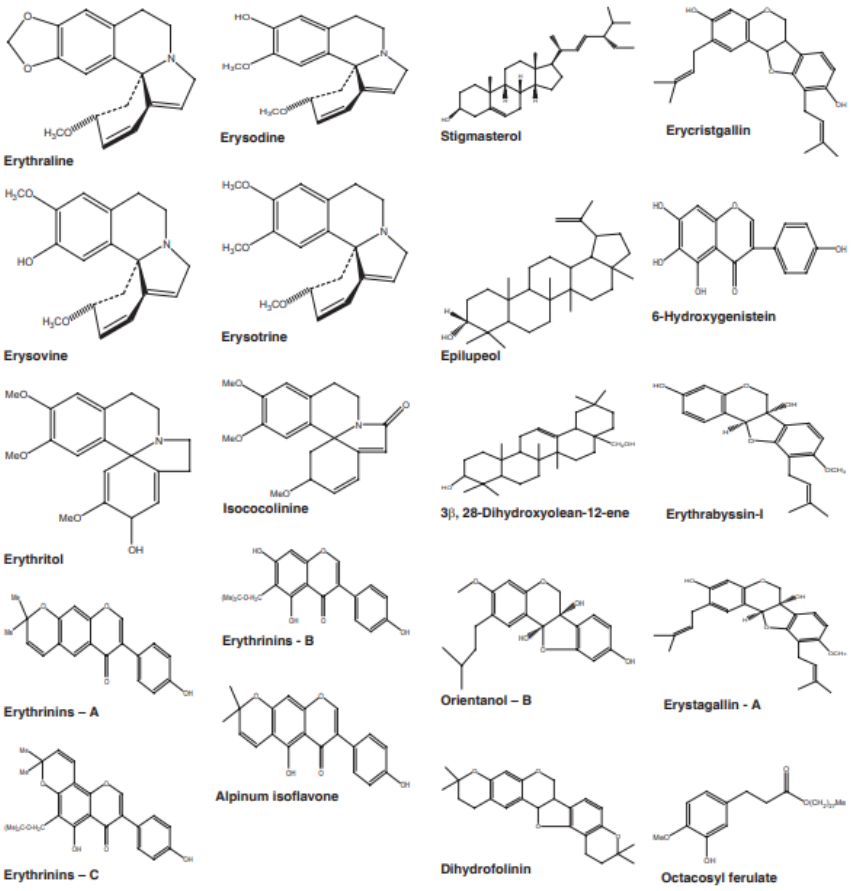

Fig. 1. Identified Phytoconstituents of E. *variegata* [12].

Additional studies have identified other bioactive compounds in the leaves and bark of *E. variegata* using liquid and gas chromatography. Fig. 2 and Table 1 highlight the gas

chromatogram and mass spectrometry analysis of the ethanolic leaf extract of *E. variegata* [16].

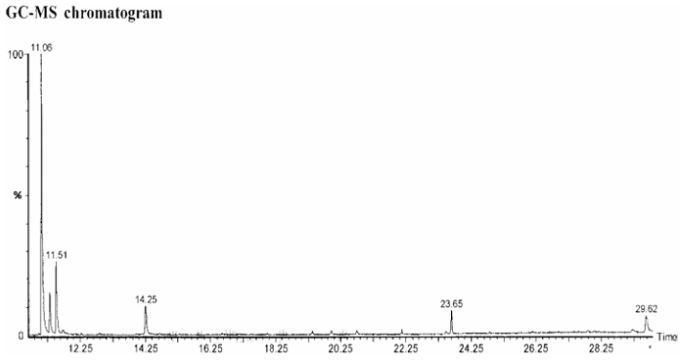

Fig. 2. Gas Chromatogram of ethanolic leaf extract of Erythrina *variegata* [16].

TABLE I

GC-MS ANALYSIS OF PHYTOCOMPOUNDS PRESENT IN THE ETHANOLIC LEAF EXTRACT OF ERYTHRINA *VARIEGATA* [16]

No.	RT	Name of the compound	Molecular formula	MW (g/mole)	Peak Area (%)
1	11.06	3-eicosyne	$C_{20}H_{38}$	278	54.93
2	11.31	3,7,11,15-tetramethyl-2-hexadecen-1-ol	$C_{20}H_{40}O$	296	7.96
3	11.51	butanoic acid, 3-methyl-, 3,7-dimethyl -6-octenyl ester	$C_{15}H_{28}O_2$	240	14.95
4	14.25	Phytol	$C_{20}H_{40}O$	296	8.02
5	19.95	1,2-benzenedicarboxylic acid, diundecyl ester	$C_{30}H_{50}O_4$	474	1.20
6	22.12	1-octanol, 2-butyl-	$C_{12}H_{26}O$	186	0.91
7	23.65	Squalene	$C_{30}H_{50}$	410	5.15
8	29.62	2H-pyran, 2-(7-heptadecynyloxy)tetrahydro-	$C_{22}H_{40}O_2$	336	6.89

MW = Molecular Weight; RT = Retention Time.

The compound 3-eicosyne is an organic terminal alkyne product found in vegetables and functions as a nutrient [17]. Butanoic acid, 3-methyl-, 3,7-dimethyl-6-octenyl ester functions as an acidulant and an arachidonic acid inhibitor. This compound also inhibits the formation of uric acid and increases the activity of the amino acid decarboxylase [18]. Phytol is a diterpene widely used as an antioxidant, antimicrobial, anti-cancer, antiarthritic, anti-diabetic, and diuretic agent [19], [20], [21]. 3,7, 11, 15-Tetramethyl-2-hexadecen-1-ol is a terpene alcohol with antimicrobial and anti-

inflammatory properties [22]. 2-H-Pyran, 2-(7-heptadecynyloxy) tetrahydro derivative is an herbicide safener and is also capable of inducing hemostatic, hepatoprotective, hemopoietic, hemolytic, and hemoglobin activities [18]. Squalene, or triterpene, is a phenolic compound and natural antioxidant most plants possess [23]. This compound has antimicrobial and chemopreventive properties protecting against colon carcinogenesis [24]. Studies have also documented its effectiveness as a gastro-preventive, hepatoprotective, pesticide, anti-tumor, and UV shield [25], [26], [27].

The authors of the same study conducted another separation experiment on the ethanolic leaf extract of *E. variegata* to isolate additional bioactive compounds using high-performance liquid chromatography (HPLC) [16]. Fig. 3 represents the HPLC chromatogram, and Table 2 illustrates the analysis of HPLC data.

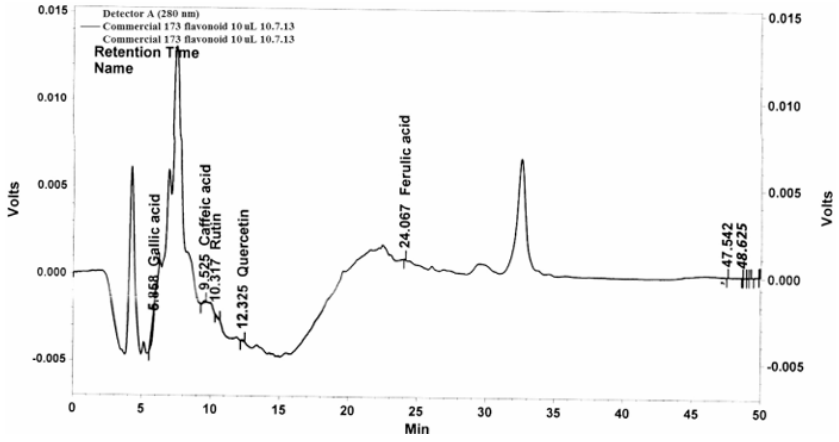

Fig. 3. HPLC chromatogram of ethanolic leaf extract of E. *variegata* [16].

TABLE II

ANALYSIS OF HPLC DATA FOR ETHANOLIC LEAF EXTRACT OF ERYTHRINA *VARIEGATA* [16]

Name	Retention time (min)	Area (%)	Height (mV)	Concentration (ppm)
Gallic acid	5.858	13,237	576	2.0
Caffeic acid	9.525	681	107	0.1
Rutin	10.317	60	0	Below detection limit
Quercetin	12.325	90	75	Below detection limit
Ferulic acid	24.067	130	32	Below detection limit

This study's HPLC chromatogram analysis documented the presence of gallic acid and caffeic acid. Gallic acid (3,4,5-trihydroxybenzoic acid) is an internal plant phenolic compound in various phytomedicines [28]. Plants rich in gallic acid exhibit hepatoprotective effects [29-31] and possess neuroprotective, antioxidant [31], anti-inflammatory [33], [34], anti-obesity [35], [36], [37], and anti-cancer properties [38]. Additionally, several other studies identified gallic acid's capability to selectively induce cancer cell apoptosis without harming healthy cells [39], [40], [41]. Another class of phenolic compounds identified in the leaves of *E.variegata* is caffeic acid, which is representative of the hydroxycinnamic acid group of compounds. Caffeic acid is known as an effective antioxidant and prooxidant [40].

A study examining the phytochemical composition of the ethanolic extract of *E. variegata* bark revealed the presence of compounds contributing to anti-depressant function. This study used LC-MS and GC-MS to isolate the bioactive compounds [42].

This study effectively expanded the phytochemical profile of *E. variegata* by identifying compounds present in a different part of the plant. Still, the authors did not specify whether the bark used for experimentation was from the stem or root. Fig. 4 illustrates the liquid chromatogram, and Table 3 represents the mass spectrum analysis for the respective chromatogram.

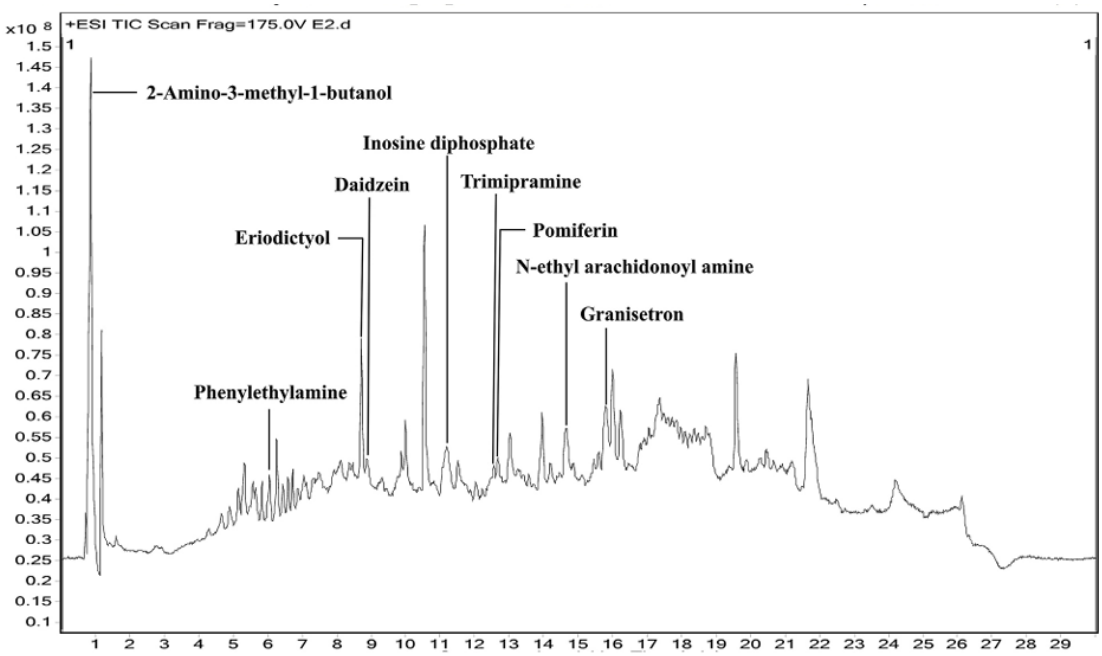

Fig. 4. Liquid chromatogram of ethanolic bark extract of E. *variegata* [41].

TABLE III

MASS SPECTROMETRY ANALYSIS OF ETHANOLIC BARK EXTRACT OF E. *VARIEGATA* [41]

Retention time	Compound	Parent *m/z*	Daughter *m/z*	Response/Abundance	Dwell (sec)	Cone (volts)	Collision energy (eV)
7.84	Inosine diphosphate	269.2	137	614.100	1	20	13
8.26	2-amino-3-methyl-1-butanol	127	77	173.640	1	66	69
8.26	Phenylethylamine	103.16	103	51587.141	1	42	1
8.26	Daidzein	254.23	133	2847.244	1	25	19
8.67	Eriodictyol	288.25	288	12298.828	1	30	1

Identified compounds showed marked effectiveness as an anti-depressant when monitoring the mechanism of action for regulating monoamine oxidase activity in mice. Other compounds identified contributing to anti-depressant effectiveness are illustrated in Fig. 5 and Table 4 [42].

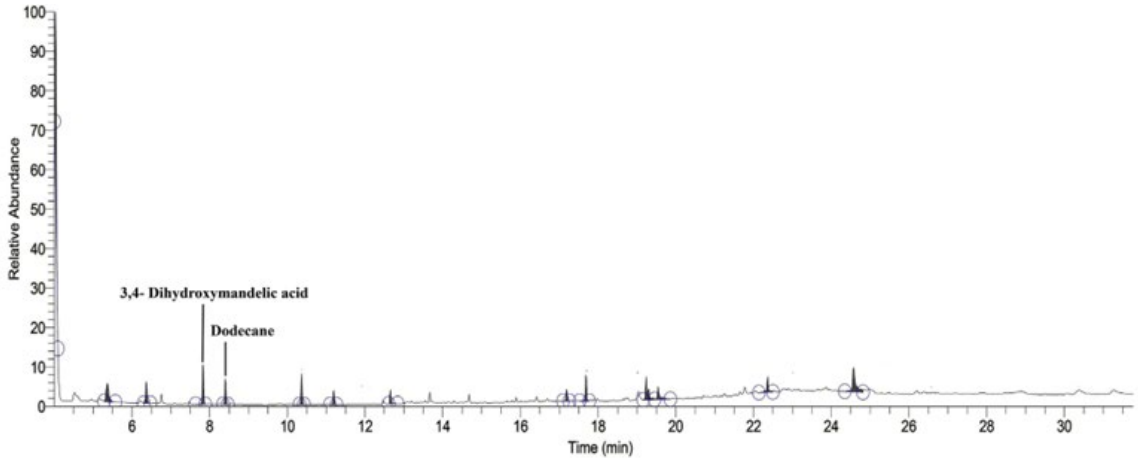

Fig. 5. Gas Chromatogram of ethanolic bark extract of E. *variegata* [42].

TABLE IV

GC-MS ANALYSIS OF ETHANOLIC BARK EXTRACT OF E. *VARIEGATA* [42]

Retention time	Compound	Molecular weight	Molecular formula
4.03	Tetrahydro-3-methyl-5-oxo-2-furancarboxylic acid	144	$C_6H_8O_4$
4.03	Ethyl 4-(ethyloxy)-2-oxobut-3-enoate	172	$C_8H_{12}O_4$
4.03	3-Methyl-isoxazol-5(4H)-one	99	$C_4H_5NO_2$
5.36	1,1,3,3,5,5,7,7-Octamethyl-7-(2methylpropoxy)tetra siloxan-1-ol	370	$C_{12}H_{34}O_5Si_4$
5.36	Cyclotetrasiloxane, octamethyl-	296	$C_8H_{24}O_4Si_4$
5.36	3-Butoxy-1,1,1,5,5,5-hexamethyl-3-(trimethylsiloxy) trisiloxane	368	$C_{13}H_{36}O_6Si_4$
6.37	2-Hexynyl aldehyde diethyl acetal	170	$C_{10}H_{18}O_2$
6.37	2,4-Hexadiene,1,1-diethoxy-	170	$C_{10}H_{18}O_2$
6.37	2,4-Hexadiene,1,1-diethoxy-,(E,E)-	170	$C_{10}H_{18}O_2$
7.82	Cyclopentasiloxane, decamethyl-	370	$C_{10}H_{30}O_5Si_5$
7.82	Benzoic acid, 2,6-bis[(trimethylsilyl)oxy]-, trimethylsilyl ester	370	$C_{16}H_{30}O_4Si_3$
7.82	3,4-Dihydroxymandelic acid, ethyl ester, tri-TMS	428	$C_{19}H_{36}O_5Si_3$
8.40	Dodecane	170	$C_{12}H_{26}$
8.40	Tetradecane	198	$C_{14}H_{30}$
8.40	Pentadecane	212	$C_{15}H_{32}$
10.37	Cyclohexasiloxane, dodecamethyl-	444	$C_{12}H_{36}O_6Si_6$
10.37	Heptasiloxane, 1,1,3,3,5,5,7,7,9,9,11,11,13,13-tetradecamethyl-	504	$C_{14}H_{44}O_6Si_7$
10.37	Octasiloxane, 1,1,3,3,5,5,7,7,9,9,11,11,13,13,15,15-hexadecamethyl-	578	$C_{16}H_{50}O_7Si_8$
11.19	Dodecane, 2,5-dimethyl-	198	$C_{14}H_{30}$
12.65	Cycloheptasiloxane, tetradecamethyl-	518	$C_{14}H_{42}O_7Si_7$
12.65	3-Isopropoxy-1,1,1,7,7,7-hexamethyl-3,5,5-tris(trimethylsiloxy) tetrasiloxane	576	$C_{18}H_{52}O_7Si_7$
12.65	Octasiloxane, 1,1,3,3,5,5,7,7,9,9,11,11,13,13,15,15-hexadecamethyl-	578	$C_{16}H_{50}O_7Si_8$
17.19	Dibutyl phthalate	278	$C_{16}H_{22}O_4$
17.19	Phthalic acid, butyl hept-4-yl ester	320	$C_{19}H_{28}O_4$
17.19	Phthalic acid, butyl hept-3-yl ester	320	$C_{19}H_{28}O_4$
17.69	Hexadecanoic acid, ethyl ester	284	$C_{18}H_{36}O_2$
17.69	Hexadecanoic acid, 2-methyl-, methyl ester	284	$C_{18}H_{36}O_2$
17.69	Ethyl 13-methyl-tetradecanoate	270	$C_{17}H_{34}O_2$
19.23	9,12-Octadecadienoic acid, ethyl ester	308	$C_{20}H_{36}O_2$
19.23	n-propyl 9,12-octadecadienoate	322	$C_{21}H_{38}O_2$
19.23	Butyl 9,12-octadecadienoate	336	$C_{22}H_{40}O_2$
19.54	Heptadecanoic acid, 15-methyl-, ethyl ester	312	$C_{20}H_{40}O_2$
19.54	Octadecanoic acid, ethyl ester	312	$C_{20}H_{40}O_2$
19.54	Ethyl 13-methyl-tetradecanoate	270	$C_{17}H_{34}O_2$
22.37	Diisooctyl phthalate	390	$C_{24}H_{38}O_4$
22.37	Phthalic acid, di(2-propylpentyl) ester	390	$C_{24}H_{38}O_4$
22.37	Bis(2-ethylhexyl) phthalate	390	$C_{24}H_{38}O_4$
24.58	13-Docosenamide, (Z)-	337	$C_{22}H_{43}NO$
24.58	trans-13-Docosenamide	337	$C_{22}H_{43}NO$
24.58	Bis(cis-13-docosenamido) methane	686	$C_{45}H_{86}N_2O_2$

TABLE V

SUMMARY OF MAJOR BIOACTIVE COMPONENTS OF E. *VARIEGATA* [43]

Compound Name	**Biological activity**
Hexadecanoic acid	Hypercholesterolemic, Lubricant, Antimicrobial, Flavor, Cosmetic and Perfumery
7,10-Hexadecadienoic acid, methyl ester	Antioxidant, anti-inflammatory, hypocholesterolemic and anti-cancer
3-eicosyne	Antimicrobial
Butanoic acid, 3-methyl-, 3,7-dimethyl -6-octenyl ester	Antimicrobial
1,3-Propanediol, 2-ethyl-2-(hydroxyl met hyl)	Antioxidant and Antimicrobial. Activities
1,2-Benzenedicarboxylic acid, dibutyl ester	Antimicrobial and Antifouling
Phytol	Anti-nociceptive, Antioxidant, anticancer, anti-inflammatory, antimicrobial, diuretic, chemo preventive properties
17-Octadecenoic acid, methyl ester	Antimicrobial and Anti-inflammatory
9,12,15-Octadecatrienoic acid, methyl ester	Anti-inflammatory, Hypocholesterolemic, anti-cancer, Hepatoprotective, Nematicide, Insectifuge, Antihistaminic, Anti-eczemic, Anti-acne, 5-Alpha Reductase inhibitor, Anti-androgenic, Anti-arthritic, Anti-coronary and Insectifuge.
2-Hexadecen-1-ol, 3,7,11,15-tetramethyl	Anti-nociceptive and antioxidant Anti-inflammatory

In conclusion, in examination of the current established phytochemical profile of *E. variegata*, Table 5 is a helpful summary of major bioactive components contributing to the healing properties of *E. variegata* and respective biological functions, confirming its traditional use and effectiveness in treating various ailments. The current research scope regarding the phytoconstituents of *E. variegata* provides a robust profile of bioactive compounds for the plant leaves. However, despite studies documenting phytochemicals in the bark, it is unclear whether samples are taken from the root or stem bark. Additionally, when examining *E. variegata* bark GC-MS analysis compared to its respective chromatogram, some compounds listed as present are difficult to differentiate from noise and possess a relatively low abundance. This thesis sought to address these issues in reporting and provide a clear illustration and analysis of bioactive compounds present in *E. variegata* through GC-MS. Additionally, the plant is not native to North America. Chromatogram analysis will confirm whether samples are *E. variegata* derivatives upon comparison with the more reputable data and analysis of *E. variegata* leaves.

2.2: Medicinal Uses:

Different parts of *E. variegata* have been used in traditional medicine as a nervine sedative, expectorant, antiseptic, antiasthmatic, antiepileptic, antiseptic, astringent, febrifuge, anti-bilious, diuretic, laxative, collyrium in ophthalmia, and anthelmintic [12],[14],[44], [45], [46], [47]. In addition to traditional medicine uses, scientists have conducted experiments testing the medicinal effectiveness of the antioxidant and cytotoxic bioactive properties of *E. variegata.* This thesis sought to enhance the bioactive

properties of *E. variegata* through synthesis of silver and titanium nanoparticles using the plant's extract.

2.2.1: Antioxidant Activity

A study conducted by Rahman and colleagues in 2010 revealed that the methanolic extract from stem bark, along with its fractions in n-hexane, carbon tetrachloride, and chloroform, demonstrated a moderate ability to neutralize DPPH radicals, with IC 50 values ranging between 82.35 and 484.4 µg/ml [14]. On the other hand, specific isolated compounds such as 4′,5,7-trihydroxy-8-prenyl isoflavone, alpinum isoflavone, and 6-hydroxygenistein exhibited significantly stronger antioxidant properties. Their IC 50 values were measured at 6.42, 8.30, and 8.78 µg/ml, respectively, indicating a higher efficacy than the extracts. These values closely aligned with the standard antioxidant, tert-butyl-1-hydroxytoluene (BUT), with an IC 50 value of 5.88 µg/ml.

Additionally, research by Sakat and Juvekar in 2010 highlighted that both aqueous and methanol extracts from leaves showed substantial DPPH radical scavenging abilities, with IC 50 values of 342.59 µg/ml and 283.24 µg/ml, respectively [48]. The ability of these extracts to scavenge nitric oxide radicals was also significant, reflected in their IC 50 values of 250.12 µg/ml for the aqueous extract and 328.29 µg/ml for the methanol extract. The aqueous extract demonstrated a more potent inhibition of lipid peroxidation, induced by thiobarbituric acid reactive substances (TBARS), with a lower IC 50 value of 97.29 µg/ml, compared to the methanol extract, which had an IC 50 value of 283.74 µg/ml. Both extracts contained similar amounts of total phenolics, while the aqueous

extract had a higher concentration of total flavonoids than total flavonols, in contrast to the methanol extract [48].

Furthermore, an additional study on the antioxidant effectiveness of *E.variegata* stem bark performed by John, Bibu, and Usha evaluated the antioxidant potential of the methanol extract of its stem bark by investigating its ability to scavenge DPPH and nitric oxide free radicals [49]. The stem bark was extracted using a Soxhlet apparatus with methanol and then concentrated under reduced pressure and temperature. Qualitative phytochemical analysis of the extract revealed the presence of various active constituents, including steroids, alkaloids, tannins, phenolic compounds, flavonoids, diterpenes, triterpenes, and saponins. The antioxidant activity was assessed through modified DPPH and nitric oxide scavenging assays. The results demonstrated that the extract exhibited scavenging activity in a dose-dependent manner. Notably, for DPPH free radical inhibition, the extract showed an EC50 value of 45.86 ± 5.85 µg/mL, comparable to vitamin C. The stem bark extract also exhibited ample efficiency compared to a vitamin C standard in the nitric oxide radical scavenging assay, with an EC50 of 28.14 ± 3.42 µg/mL. The presence of phenolics and flavonoids, known for their free radical scavenging properties, was confirmed, supporting the extract's traditional medicinal use. This study conclusively demonstrated the in vitro antioxidant activity of *E. variegata* stem bark methanol extract, highlighting its potential therapeutic benefits. However, errors in data analysis reporting for this study leave the reader unsure if the experiments maintained accuracy and precision, as the authors do not mention if the experiments were repeated. The work conducted in this thesis sought to enhance the reported antioxidant

activity of *E. variegata* by conducting experiments testing DPPH and nitric oxide scavenging capability while maintaining accuracy and precision.

2.2.2: Cytotoxic Activity

While there is no present research regarding the use of *E. variegata* root bark extract or silver or titanium nanoparticles synthesized using *E. variegata* root bark in an MTT (3-(4,5-dimethylthiazol-2-yl)-2,5-diphenyltetrazolium bromide assay, there have been studies documenting the cytotoxic effects of the plant in anti-cancer studies. In 2006, Li et al. found that the ethyl acetate and n-butanol fractions of the ethanolic stem bark extract of *E. variegata*, but not its aqueous fraction, promoted the proliferation of rat osteogenic sarcoma (UMR106) and osteoblast-like cells [50]. The study identified 11 compounds in the ethyl acetate fraction, including four new isoflavones and seven known compounds, such as euchrenone b 10 and isoerysenegalensein E, which stimulated UMR106 cell proliferation at concentrations ranging from 5×10^{-8} to 5×10^{-6} mol/L. However, these compounds did not promote proliferation at a higher 5×10^{-5} mol/L concentration.

Further, Ohba et al. discovered that among the proteinase inhibitors from E. *variegata*, EBI, a member of the Bowman-Birk family of inhibitors, was cytotoxic in T lymphoblastic leukemia (T-ALL) cells, specifically Molt4 and Jurkat cells, while Kunitz family inhibitors ETIa and ECI were not [51]. The study also found that the succinylation of lysine residues in EBI resulted in a 50% reduction in trypsin inhibitory activity and a loss of cytotoxicity in Molt-4 cells.

In other studies, Herlina et al. reported that an *Erythrina* alkaloid derivative, 10,11-dioxoerythratidine, isolated from the leaves, and the methanol leaf extract, along

with its ethyl acetate fraction and two compounds, exhibited anti-cancer activity against the breast cancer cell line T47D in vitro [52]. The compounds were more potent than the extracts, with isolate 17 being the most effective, followed by isolate 11, the ethyl acetate fraction, and the methanol extract. Isolate 11 was identified as a triterpene pentacyclic compound and isolate 17 as a mixture of β-sitosterol and stigmasterol.

Rahman et al. evaluated the cytotoxicity of various fractions of the methanol bark extract of E. *variegata* against brine shrimp and Artemia salina [53]. In this study, researchers discovered significant toxicity, particularly in the carbon tetrachloride and chloroform soluble fractions, suggesting their potential as antiproliferative and antitumorous agents. Additionally, Zhang et al. demonstrated the anti-tumor effects of *E. variegata* extract in vivo using a Lewis lung cancer mouse model and in vitro against liver cancer cells [54]. Herlina et al. further confirmed the significant anti-cancer activity of the methanol stem bark extract against breast cancer T47D cell lines in vitro. The bioactive component, erystagallin A, showed potent activity with an IC50 of 3.3 µg/ml [55]. Finally, Rasul et al. found that xanthoxyletin, isolated from E. *variegata*, exhibited antiproliferative effects against human gastric adenocarcinoma SGC-7901 cells, inducing DNA damage, apoptosis, and cell-cycle arrest while also increasing reactive oxygen species production [56]. Baskar et al. reported that treatment with the methanol root bark extract of Erythrina *variegata* significantly increased lifespan, reduced cancer cell number and tumor weight, and normalized hematological parameters in mice with Dalton's ascitic lymphoma [57].

2.3 Rising Human and Environmental Health Concerns

Free radicals are necessary for regulating critical physiological functions like immune defense and cellular signaling at moderate levels. However, the overproduction or insufficient neutralization of free radical reactive oxygen species (RNS) or reactive nitrogen species (RNS) by antioxidants leads to oxidative and nitrosative stress, causing potential damage to critical biomolecules such as nucleic acids, proteins, and lipids and is known to cause cellular death [58], [59], [60] ROS and RNS are derived from both endogenous sources such as mitochondria, endoplasmic reticulum, peroxisomes, and phagocytic cells and exogenous sources such as pollution, tobacco smoke, heavy and transition metals, industrial solvents, pesticides, alcohol, and certain drugs like halothane and paracetamol, and radiation [61]. Tables 6 and 7 reference ROS species generated endogenously and exogenously, respectively.

The accumulation of ROS and RNS alters the normal cellular redox status, leading to increased oxidative stress. Free radical-induced oxidative stress is implicated in several diseased conditions such as diabetes mellitus, Parkinson's disease, Alzheimer's disease, Multiple sclerosis, atherosclerosis, hypertension, asthma, cataract development, rheumatoid arthritis, and various cancers [61].

TABLE VI

ENDOGENOUS SOURCES OF ROS/RNS [61]

Enzyme	Substrate	ROS
Acyl CoA-oxidases (enzymes of β-oxidation)	Fatty acids	H_2O_2
D-amino acid oxidase	D-proline	H_2O_2
L-α-hydroxy oxidase	Glycolate	H_2O_2
Urate oxidase	Uric acid	H_2O_2
D-aspartate oxidase	D-aspartate	H_2O_2
Xanthine oxidase	Xanthine	$O_2^{\bullet -}$, H_2O_2

TABLE VII

EXOGENOUS SOURCES OF ROS/RNS [61]

Air & water pollution	Ultraviolet light
Alcohol	Cooking (smoked meat, used oil, fat)
Tobacco smoke	Drugs such as
Transition metals- Cd, Hg, Pb, As	Halothene, Paracetamol,
Heavy metals- Fe, Cu, Co, Cr	Bleomycine, Doxorubicin,
Industrial solvents	Metrenidazole, Ethanol.
Pesticides	CCl_4
High temperature	

The accumulation of ROS and RNS contributes to the progression of various diseases. Therefore, limiting excess exposure to exogenous sources of free radical species is essential. The current drastic decrease in atmospheric conditions due to human activities such as fuel combustion, transportation, and smoking contributes to the release of vast amounts of nitrogen, sulfur, and carbon oxides, all resulting in the increased presence of ROS and RNS [8]. Therefore, there is a need to address free radical species on the molecular level for human health and the atmospheric level for environmental

health. This thesis sought to use the DPPH and nitric oxide radical scavenging assays to obtain knowledge that could address the issue of oxidative stress on the molecular and environmental levels, which will enhance human and environmental health. In an attempt to improve the present bioactive properties of *E. variegata* by using its' root bark extract to synthesize silver and titanium nanoparticles, this work hoped to provide a foundation for future use of this plant and synthesized nanoparticles for applications in the remediation of air and water pollution and drug delivery.

2.4 Nanotechnology

The field of nanotechnology is currently one of the most widely expanding areas of research. Nanoparticles possess unique physiochemical properties, allowing them to be at the interface of chemistry, engineering, medicine, and physics. The current state of nanotechnology research encompasses using nanoparticles in materials science, electronics, biomedicine, and pollution control. The formation of nanoparticles is often the product of green, chemical, or physical synthesis. These methods can be categorized into top-down or bottom-up approaches, as illustrated by Fig. 6 [62]. With chemical and physical processes of synthesis often requiring large amounts of radiation and highly concentrated stabilizing and reducing agents that are harmful to the environment, the synthesis of nanoparticles using plants, bacteria, and algae, widely referred to as green synthesis, has gained considerable popularity [63].

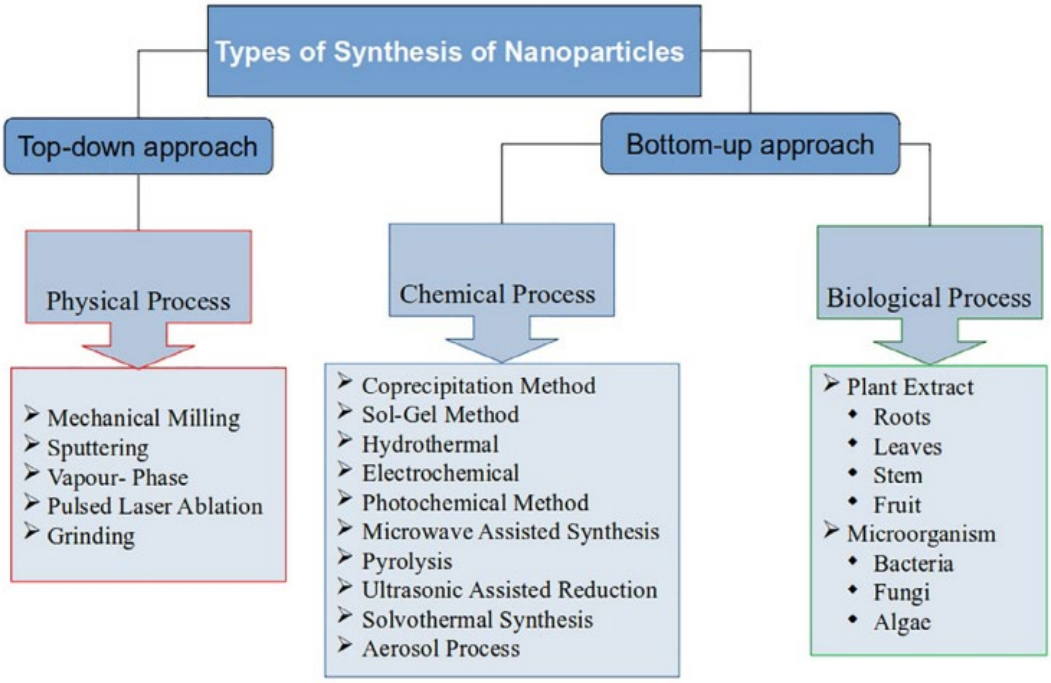

Fig. 6. Methods for Nanoparticle Synthesis [63].

One of the most notable fields of nanoparticle research explores their use in drug delivery. Research reveals that an overwhelming amount of conventional drugs possess limited bioavailability and aqueous solubility, reducing their capacity for absorption and retention within biological systems, causing researchers to make significant strides in identifying methods to improve the efficiency of many traditional/conventional drugs [64]. Many nanoparticles are believed to have enhanced pharmacokinetic abilities due to their physical nature and reduced size. Depending on the particle type, these structures can target specific cells for selective action. Nanoparticles can easily penetrate target cells and then aggregate in subcellular structures to modify cellular processes, which can be beneficial in treating chronic diseases such as cancer, kidney disease, and diabetes [65]. While nanoparticles represent a solution to issues presented by conventional drugs, there are concerns regarding the cytotoxicity of these materials. Different findings have shown

that the mechanism of nanoparticle size-dependent cytotoxicity is the result of their ability to infiltrate body tissues and, subsequently, cells and modify crucial cellular functions, one of which causes the rupture of the membrane of subcellular structures and induces the overproduction of reactive oxygen species (ROS) [66]. Additionally, nanoparticles' shape and aspect ratio are crucial in their cytotoxic effects in vivo. Scientists have noted that an increased aspect ratio of nanoparticles is directly related to cytotoxicity due to reduced clearance and increased bioavailability of nanoparticles [67].

Nanotechnology has also gained traction in water and air pollution remediation. With only 30% of the water on Earth not confined to ice and glaciers and a minuscule 0.08% of that being safe for consumption, implementing technologies to address the scarcity of clean water is increasingly necessary [68]. Nanotechnology offers promising solutions to enhance water quality with various nanotechnology-based methods, including reactive media for separation and filtration, bioremediation, and disinfection, which are being explored [69], [70], [71]. Remediation involves strategies to eliminate, reduce, or neutralize water pollutants threatening human health and ecosystems. Nanomaterials often exhibit enhanced affinity, capacity, and selectivity for heavy metals and other contaminants, offering advantages such as increased reactivity, greater surface area for contact, and improved disposal capabilities, allowing for the creation of nanofiltration membranes for water purification, which have demonstrated marked effectiveness in reducing bacteria and heavy metal content in water [68].

Scientists have also begun imploring the use of metal oxide nanoparticles for air pollution remediation by using them as photocatalysts. Materials like titanium dioxide (TiO_2), zinc oxide (ZnO), iron (III) oxide (Fe_2O_3), and tungsten oxide (WO_3) are known

for their photocatalytic properties. These photocatalysts have a range of applications, including their use as a white pigment in paper and paint, as a UV light-absorbing component in sunscreens, and in protective antimicrobials and self-cleaning products. In the context of environmental protection and water remediation, these photocatalysts can effectively convert organic pollutants into harmless substances. Most notable is the application of TiO_2 in sophisticated photochemical oxidation processes for water purification due to its non-toxic nature, superior photoconductivity, photostability, widespread availability, and cost-effectiveness [72].

Titanium dioxide and silver nanoparticles are the chosen nanomaterials for the work in this thesis. TiO_2 and silver nanoparticles were selected because research demonstrates their capacity to enhance antioxidant enzymes, exhibit cytotoxicity effects on cancer cell lines, and absorb and filter air and water pollutants while maintaining relatively low toxicity levels, though titanium is less toxic [72], [73]. There is currently only one peer-reviewed article outlining the synthesis of nanoparticles using *E. variegata.* This research article focused on synthesizing zinc oxide nanoparticles using the *E.variegata* leaf extract and tested antibacterial, antioxidant, anti-inflammatory, and anti-diabetic efficacy [74]. The findings reveal that ZnO nanoparticles synthesized using the plant's leaf extract exhibit potent antibacterial properties against both Gram-negative and Gram-positive bacteria, with Minimum Inhibitory Concentration (MIC) and Minimum Bactericidal Concentration (MBC) values around 150-175 μg/mL.

Additionally, the nanoparticles showed significant antioxidant activity, with a scavenging activity IC50 value of 32.50 μg/mL and maximum activity of 94% at an 80 μg/mL concentration. The nanoparticles also possessed notable anti-inflammatory

potential, demonstrating an inhibition of protein denaturation with an IC50 value of 222.01 µg/mL. Moreover, the study highlighted the anti-diabetic potential of these nanoparticles, evidenced by their pancreatic α-amylase inhibition, with an IC50 value of 254.01 µg/mL. Compared to chemically synthesized ZnO nanoparticles, the green synthesized ones exhibited better or comparable bioactive properties in all tested activities. The study provided promising results for nanoparticles synthesized using *E.variegata*. It demonstrated that resultant nanomaterials were non-toxic and showed advantageous bioactive properties that could potentially be applied in biomedical fields as alternative therapeutic agents.

Ultimately, the nanoparticles synthesized in this work sought to enhance current research findings regarding the synthesis of nanoparticles using *E. variegata* through successfully synthesizing silver and titanium nanoparticles utilizing the plant's root bark extract and testing their ability to enhance the plant's current antioxidant and cytotoxic properties.

2.5 Cyclic Voltammetry

Cyclic voltammetry (CV) is an electrochemical technique widely used for investigating oxidation and reduction processes of molecular species. In reference to the cyclic voltammetry guide published by Elgrishi et al., this technique is commonly used in the study of electron transfer-initiated reactions, including catalysis [74]. CV measures the relationship between the electrical potential and current within a system, providing insights into the electrochemical properties of substances, such as their redox potential and reaction kinetics. A typical CV experiment involves an electrochemical cell with three electrodes: a working electrode where the reaction of interest occurs, a reference

electrode to provide a stable potential against which measurements are made, and a counter electrode to complete the circuit. The output of a CV experiment is a voltammogram, which plots current (i) versus applied potential (E). Key features include peak current, which correlates with the concentration of the analyte, and peak potential, which provides information about the redox potential of the analyte. Additionally, the selected scan rate affects the shape of the voltammogram and the peak currents. Understanding the relationship between scan rate and peak current allows for the analysis of diffusion coefficients and reaction kinetics. Beyond basic electrochemical research, CV has applications in sensor development, battery and fuel cell technology, and the study of biological systems.

This thesis explored the electrochemical properties of aqueous *E. variegata* root bark extract and the green synthesized titanium and silver nanoparticles. There is no known reduction reaction for the root bark extract. Still, when conducting electrochemical studies, it is necessary to consider the reduction reactions and potentials for silver and titanium, as demonstrated by Fig. 7.

Silver	E° (V)
$Ag^+ + e^- \rightleftharpoons Ag(s)$	0.7996
Titanium	E° (V)
$Ti^{2+} + 2e^- \rightleftharpoons Ti(s)$	−0.163

Fig. 7: Reduction reactions and potentials for silver and titanium [75].

2.6 The DPPH assay

The measure of antioxidant effectiveness in this thesis was marked by efficiency in the DPPH radical scavenging assay. DPPH is a stable free radical known for its paramagnetic properties and frequent application in electron spin resonance experiments. A study performed by Blois identified that upon accepting an electron or hydrogen in radical form, this compound can transition into a stable, diamagnetic molecule [77]. This molecule shows a strong absorption at 517 nm, and prepared solutions of DPPH are a deep violet color. As this free electron becomes paired off, the absorption decreases, and there is an observant decolorization of the DPPH solution with respect to the stoichiometric number of electrons taken up. Fig. 8 represents the reaction schema of several oxidizable groups and DPPH.

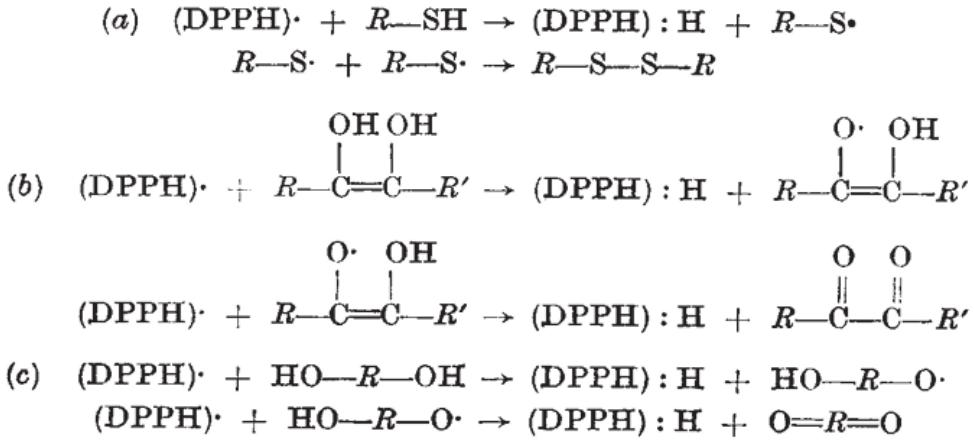

Fig. 8. Reaction schema of DPPH and oxidizable groups: (a) sulfhydryl groups, (b) conjugated ascorbic acid, (c) hydroquinone [77].

As mentioned in section 2.2.1, previous studies have been performed documenting the efficiency of E. *variegata* alone. This work will confirm if synthesized silver and titanium nanoparticles can enhance the plant's natural antioxidant capabilities.

2.7 The Nitric Oxide Assay

In this study, the antioxidant capability of synthesized titanium and silver nanoparticles was measured by the ability to scavenge the nitric oxide free radical in a nitric oxide assay. This assay involved the generation of nitric oxide from sodium nitroprusside and its measurement using the Griess reaction, a method previously described by Green et al. and Marcocci et al. [78], [79]. In this process, sodium nitroprusside in an aqueous solution at physiological pH spontaneously generates nitric oxide, which reacts with oxygen to form nitrite ions. These ions are then estimated using the Griess reagent, which forms a purple azo product due to the diazotization of nitrite ions with sulphanilamide and subsequent coupling with naphthylethylenediamine dihydrochloride. The effectiveness of nitric oxide scavenging is then measured by the absorption of the purple azo product at 546 nm.

2.8 The MTS Assay

The MTS assay, a prominent method for assessing cell proliferation and viability, functions through the reduction of MTS by dehydrogenase enzymes [79], [80]. This assay quantitatively measures cell viability by evaluating the reductive activity of cellular oxidoreductase enzymes, which convert the tetrazolium dye MTS into insoluble formazan crystals, illustrated by Fig. 9 [80].

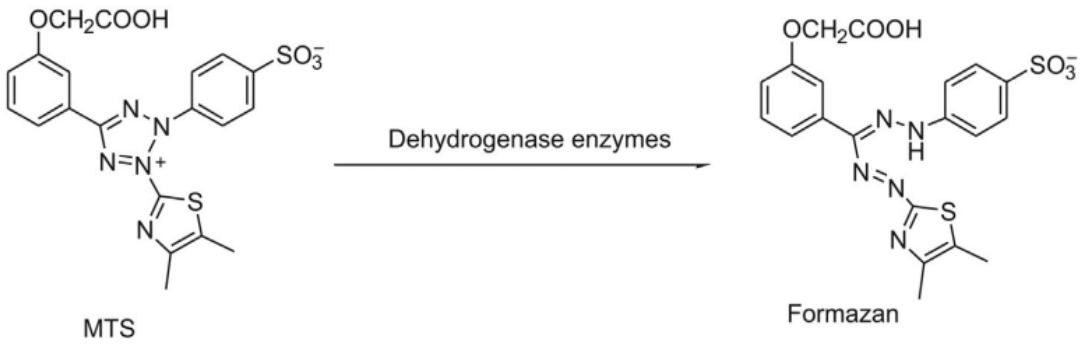

Fig. 9. Reduction of MTS to formazan [80].

In practice, this conversion is facilitated by dehydrogenases present in living cell mitochondria, though other organelles also contribute. In the presence of phenazine methosulfate (PMS), viable cells can reduce MTS to a soluble formazan product. This conversion is believed to occur through the action of NADPH-dependent dehydrogenase enzymes in metabolically active cells, and the resultant formazan dye can be quantified by measuring its absorbance at wavelengths between 490–500 nm [81].

3. METHODOLOGY

3.1 Synthesis of aqueous E.variegata root bark extract

E. variegata root bark was obtained from an apothecary in China from a region where the plant is native. Fifteen grams of bark were weighed out, washed thrice with distilled water, and air-dried. Once dried, the bark was ground into a fine powder using a Ninja Food Processor. The powder was then transferred to a beaker where 100 mL of distilled water was added. The bark was boiled at 65 degrees Celsius for 30 minutes. After boiling, the liquid was allowed to cool for 10 minutes and filtered through gravimetric filtration using Whatman #1 110 mm qualitative filter paper. Once filtration was complete, a portion of the aqueous root bark was transferred to an amber bottle and stored at 4 degrees Celsius to preserve the bioactive compounds. The other portion of the aqueous root bark extract was concentrated under rotary evaporation to obtain a solid mass for antioxidant and cytotoxicity assays.

3.2 Synthesis of the methanolic E. variegata root bark extract

The methanolic *E. variegata* root bark extract was obtained using the procedure outlined by Muthukrishnan et al. [16] with minor modifications using Soxhlet extraction. The extraction used 15 grams of powdered E. *variegata* root bark and 250 mL of methanol. The extraction ran independently until the solvent could not extract any more of the root bark. Once the extraction was complete, the resultant extract was stored at 4 degrees Celsius to preserve the bioactive compounds present.

3.3 Confirmation of Erythrina Species through GC-MS

The purity of the root bark was confirmed using the methanolic root bark extract in GC-MS analysis. The Bruker 436-GC and the Bruker EVOQ Triple Quadropole Mass Spectrometer were used to determine the phytochemical compounds of the methanolic root bark extract. The GC-MS parameters included using Agilent DB 5-MS (30m x 0.25 mm x 0.25 um, Agilant p/n 122-5532) column in a modified experimental procedure of the one performed by Muthukrishnan et al..[16] Helium gas was used as the carrier gas at a flow rate of 1 mL per minute. After a clear baseline was obtained, a 1 uL aliquot of the methanolic extract was injected into the chromatographic column. The injector temperature was 250 degrees Celsius, and the oven temperature remained 110 degrees Celsius for 2 minutes. The oven temperature was then ramped up to 280 degrees Celsius at 8 degrees Celsius per minute. The temperature was held at 280 degrees for 30 minutes, and the total runtime was 51.25 minutes. The resulting chromatogram peaks were analyzed using mass spectrometry, and the masses were compared to previous literature to identify the phytochemical constituents present in *E. variegata* through GC-MS.

3.4 Green Synthesis of EvAgNPs

Silver nanoparticles were synthesized using the aqueous root bark extract of *E. variegata***.** A 1:9 ratio solution of aqueous root bark extract and 1mM silver nitrate was used to obtain silver nanoparticles through microwave synthesis using the CEM Discover 2.0 microwave synthesizer. The solution was run in the microwave synthesizer at 90 degrees Celsius and 15 psi for 15 minutes [82]. Silver nanoparticle formation was observed by the change in the color of the solution from light yellow to dark brown. For

experimentation, silver nanoparticles were collected after centrifugation at 6000 rpm, and nanoparticles were washed twice with distilled water to remove silver nitrate solvent.

3.5 Green Synthesis of EvTiNPs

In a modified procedure of the one reported by Van Tonder et al. [83], TiO_2 nanoparticles were prepared using a green method. 23 mL of tertbutile titanate ($C_{16}H_{36}O_4Ti$) was dissolved in 23 mL of ethanol and stirred for 15 minutes. Then, 23 mL of aqueous *E. variegata* root bark extract was added dropwise to the solution under stirring until total precipitation. The mixture was then kept in an incubator oven for drying overnight at 80 degrees Celsius to evaporate the solvent.

3.6 Characterization of NPs

The characterization of EvAgNPs and EviNPs was done using UV-visible spectroscopy (UV), Fourier Transform Infrared Spectroscopy (FTIR), Scanning Electron Microscopy (SEM), Energy Dispersive X-ray Spectroscopy (EDS), and Dynamic Light Scattering (DLS).

3.6.1 UV-visible Spectroscopy

UV-visible spectroscopy was used to confirm the formation of silver and titanium nanoparticles from *E.variegata* root bark extract, and each solution was scanned using the ThermoScientific Genysys 150 UV-visible spectrometer. For each sample, a 1-cm quartz cuvette containing 2 ml of distilled water was used as a blank; then, the absorbance scan for each nanoparticle solution was obtained. The absorbance scan parameters were set from 200 to 800 nm.

3.6.2 Fourier Transform Infrared Spectroscopy (FTIR)

The FTIR measurement data was recorded using the JASCO FT/IR-4600. The FTIR parameters were set to scan from 4000-400 cm^{-1}. The aqueous *E. variegata* root bark extract, EvAgNPs, and EvTiNPs were tested to identify functional groups and chemical bonds present in each sample. Each sample was applied directly to the diamond crystal, and the spectra were recorded using the attenuated total reflection (ATR) method.

3.6.3 Cyclic Voltammetry

The electrochemical properties of the aqueous *E. variegata* root bark extract, EvAgNPs, and EvTiNPs were obtained using the BASI Epsilon C3 stand model serial # C3 1532S to measure each sample's oxidation and reduction potentials. The EvAgNPs and EvTiNPs were dissolved in distilled water to create a suspension and then briefly vortexed to ensure adequate distribution of the nanoparticles in the solution. The resulting solution for each was used to coat the surface of the carbon working electrode. Platinum and silver electrodes were also used during each experiment and served as the counter and reference electrodes. All electrodes were placed in a tris-HCl buffer solution in one experiment. Then, the experiment was repeated using a phosphate buffer solution to compare the effects of different buffer solutions on the electrochemical properties of the silver and titanium nanoparticles.

The experimental parameters for measuring the electrochemical potential of the aqueous root bark extract in phosphate buffer were set to -2280 mV for the initial and final potential, with a switching potential of 2280 mV. The scan rate was set to 100 mV per second, and the current full scale was set to 10 mA, with a filter of 10 Hz and a quiet time of 2 seconds. The experimental parameters were set to an initial and final potential

of -3200 mV for the aqueous root bark in tris-HCl buffer. The switching potential was 2900 mV. The scan rate, current full scale, filter, and quiet time remained unchanged for all experiments with the aqueous root bark, EvAgNPs, and EvTiNPs.

The initial and final potentials for the EvAgNP CV experiment in phosphate buffer were -1900 mV. The parameters for the EvAgNPs in the tris-HCl buffer were an initial and final potential of -2000 mV and a switching potential of 2100 mV. The initial and final potentials for the EvTiNPs in phosphate buffer were -1825 mV, and the switching potential was 2000 mV. The parameters for EvTiNPs in tris-HCl were set to an initial and final potential of -1740 mV and a switching potential of 2000 mV.

3.6.4 Scanning Electron Microscopy (SEM) & Energy Dispersive X-ray Spectroscopy (EDS)

SEM and EDS analyses were performed using the JEOL JSM- 6010 LA scanning electron microscope and In TouchScope software. The backscattered electron images were collected using an accelerating voltage of 10 kV and a working distance of 9 mm. For the EvAgNPs, backscattered images were also taken at 7 kV. The EDS spectra were taken at a magnification of 200X and 1000X for the EvAgNPs and 3000X and 8000x for the EvTiNPs.

3.6.5 Dynamic Light Scattering

Silver and titanium nanoparticle size was measured by dynamic light scattering using the Anton Paar Litesizer 500 instrument at 25 degrees Celsius. Before measurement, 200 ug/mL solutions of EvAgNPs and EvTiNPs in distilled water were sonicated for 15 minutes. Following sonication, each solution was filtered using a 0.2-

micron filter and then diluted by a factor of 100. Then, each measurement was taken using a 1-cm cuvette.

3.7 The DPPH Assay

The 1,1-Diphenyl-2-picryl-hydrazyl (DPPH) assay was performed following the protocol of Anjana et al. [82] with minor modifications to measure free radical scavenging activity was measured. The solutions tested were ascorbic acid, *E. variegata* root bark extract, EvAgNPs, and EvTiNPs, each dissolved in methanol. The concentrations of tested solutions were 25, 50, 100, and 200 ug/mL. Each solution contained 1 mL of sample and 1 mL of DPPH and then was incubated in the dark at room temperature for 30 minutes. A control of methanol alone and DPPH was used for each experiment. After 30 minutes, the samples containing nanoparticles were centrifuged at 5000 rpm for 5 minutes at 25 degrees Celsius to obtain an accurate baseline. Then, each sample's absorbance was read at 517 nm using the ThermoFisher Genysys UV-Visible Spectrometer and compared to the absorbance of the control. Silver nitrate and titanium dioxide controls were also run to ensure that any detected scavenging ability resulted from the EvAgNP or EvTiNP sample, not the solvent.

Antioxidant effectiveness was determined by the inhibition ratio value, which is determined by the equation illustrated in Fig. 9, where A_0 is the absorbance of the control, and A_c is the absorbance of the sample.

$$\text{Inhibition ratio } (\%) = \{(A_0 - \text{Ac})/A_0\} \times 100$$

Fig. 10. Inhibition Ratio Calculation.

3.8 The Nitric Oxide Assay

The nitric oxide scavenging activity of *E. variegata* root bark extract, ascorbic acid, EvAgNPs, and EvTiNPs were measured. Each sample was dissolved in methanol, and 25, 50, 100, and 200 ug/mL concentrations were tested. Following John et al.'s procedure with minor modifications [49], 250 uL of 5 mM sodium nitroprusside made in phosphate-buffered saline (PBS) was added to 1 mL of sample and incubated for 2 hours at 25 degrees Celsius. After incubation, 600 uL of Griess reagent (1% sulfanilamide in 5% orthophosphoric acid and 0.1% naphthyethylene-diamine-dihydrochloride in distilled water) was added to the reaction mixture. The absorbance of the solution was read at 546 immediately following the addition of the Griess reagent against a methanol blank and compared to a Vitamin C standard. The effectiveness of each sample's nitric oxide scavenging ability was determined using the inhibition ratio calculation illustrated in Fig. 10.

3.9 The MTS Assay

The MTS assay was used to determine cell viability by evaluating the reductive activity of cellular oxidoreductase enzymes. Samples tested using this assay included the aqueous *E. variegata* root bark extract, EvTiNPs, and titanium dioxide (TiO_2) as a control. Silver was not tested in this assay due to its limited yield and large sample requirement for the assay. The cytotoxicity of each sample was measured in the assay based on the loss of viable cells. The cells used in this assay were from the H358 cell line, which are bronchioalveolar carcinoma, non-small lung cancer cells. Samples were monitored for five days, and the absorbance was taken at 490 nm.

4. RESULTS

4.1 Synthesis of aqueous E. variegata root bark extract

Fig. 11 outlines the procedure for synthesizing the aqueous *E. variegata* root bark extract. The bark was washed, dried, crushed, boiled, and then filtered to obtain the extract used for experimentation.

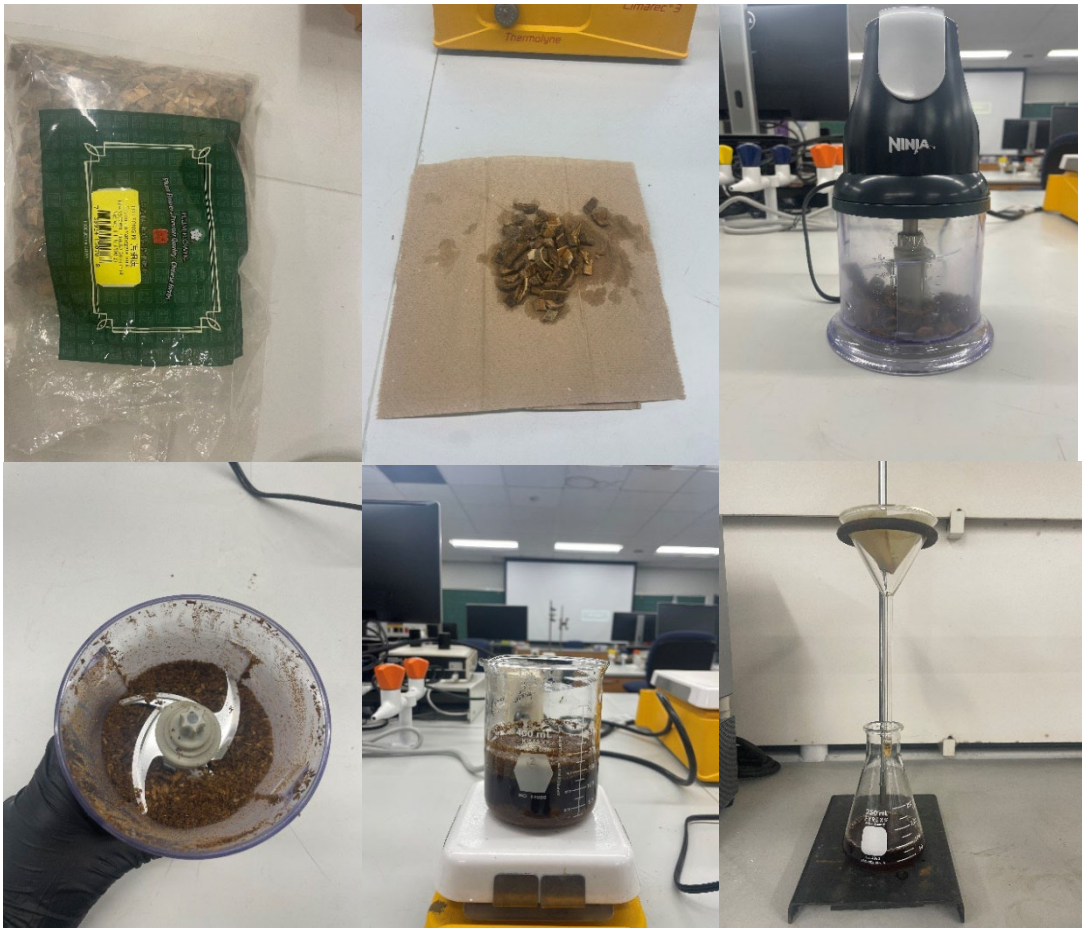

Fig. 11. Aqueous E. *variegata* root bark extraction procedure.

4.2 Synthesis of the methanolic E. variegata root bark extract

Fig. 12 demonstrates the synthesis of the methanolic *E. variegata* root bark extract using the Soxhlet apparatus.

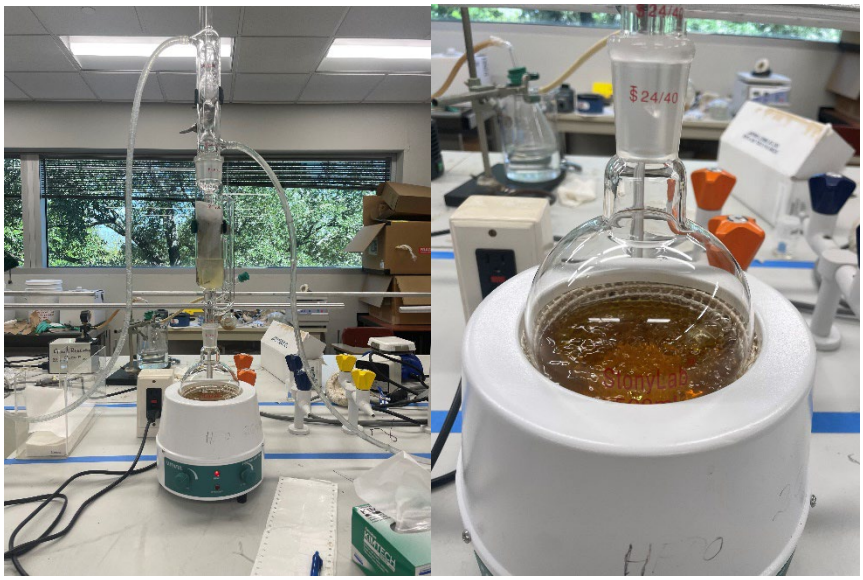

Fig. 12. Synthesis of methanolic E. *variegata* root bark extract using Soxhlet extraction.

4.3 Confirmation of Erythrina species through GC-MS

Fig. 13 and Table 8 represent the data obtained through GC-MS experiments. Fig. 13 shows the chromatogram for the methanolic extract of *E. variegata* with observable peaks at 6.240, 8.790, 11.177, 13.281, 15.151, 16.80, 18.409, 19.839, and 21.188 min(s). Fig. 8 presents the GC-MS analysis of compounds in the tested methanolic root bark extract using literature documenting the phytochemical profile of different parts of the *E. variegata* plant using GC-MS. The biological function of the phytochemical compounds is also listed.

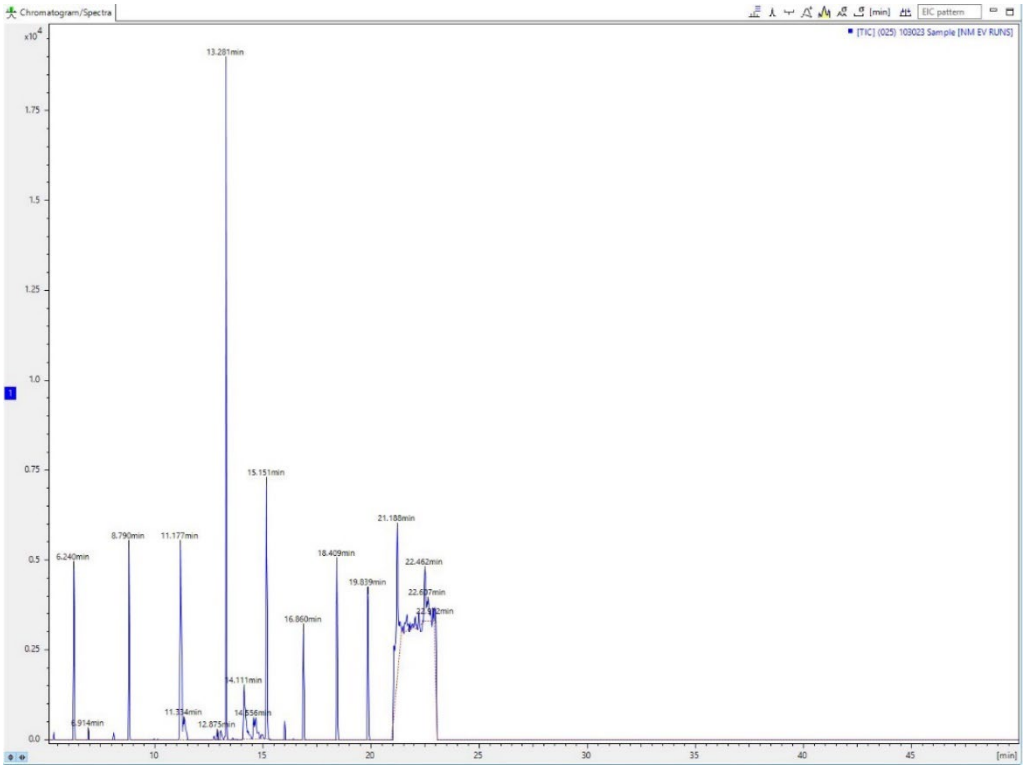

Fig. 13. Gas chromatogram of methanolic E. *variegata* root bark extract.

TABLE VIII

IDENTIFIED COMPOUNDS PRESENT IN METHANOLIC E. *VARIEGATA* ROOT BARK EXTRACT AND THEIR BIOLOGICAL FUNCTIONS

Retention time (min)	Name of the compound	Molecular formula	m/z	Biological function
8.79	3-eicosyne	$C_{20}H_{38}$	279.52	Antimicrobial
11.177	3, 7, 11, 15-tetramethyl-2-hexadecen-1-ol	$C_{20}H_{40}O$	296.51	Antimicrobial & Antiinflamm-atory
13.278	Phytol	$C_{20}H_{40}O$	296.72	Antimicrobial, Antioxidant, Anti-tumor, Anticancer, antiarthritic, anti-diabetic, chemopreventive
15.151	2-hexadecen-1-ol, 3,7,11, 15-tetramethyl-	$C_{20}H_{40}O$	296.69	Anti-nociceptive, Antioxidant. Anti-inflammatory
16.86	1,2-benzenedicarboxylic acid, diundecyl ester	$C_{30}H_{50}O_4$	475.52	Antimicrobial. Antifouling
21.188	1-octanol, 2-butyl	$C_{12}H_{26}O$	189.38	Antimicrobial

4.4 Green Synthesis of EvAgNPs

Fig. 14 and 15 illustrate the green synthesis of the EvAgNPs. In Fig. 14, picture A represents the silver nitrate and aqueous *E. variegata* extract solution before microwave synthesis, and picture B represents the solutions after microwave synthesis. Fig. 15 depicts the dried EvAgNPs from the microwave-synthesized *E. variegata* and silver nitrate solution following centrifugation and washing.

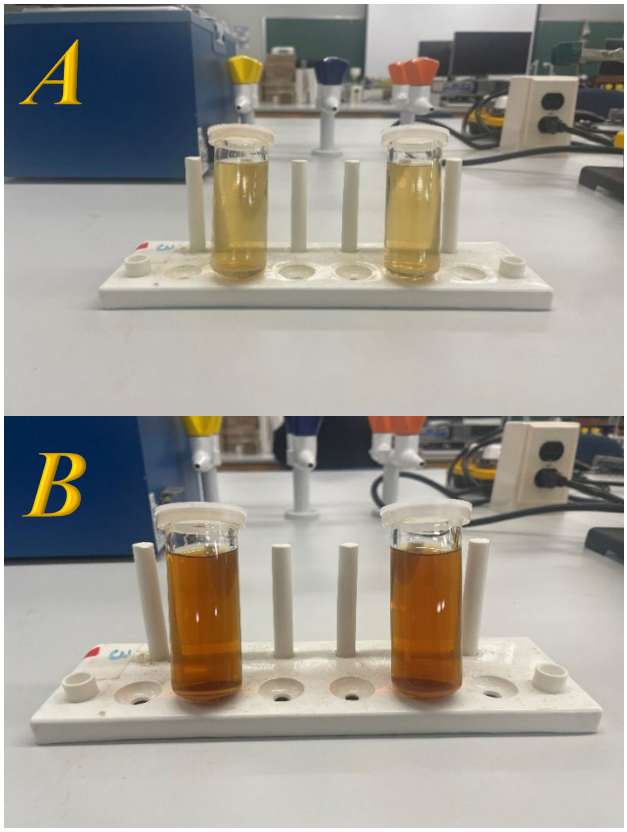

Fig. 14. Synthesis of EvAgNPs (a) before microwave synthesis and (b) after microwave synthesis.

Fig. 15. Dried EvAgNPs.

4.5 Green synthesis of EvTiNPs

Fig. 16 illustrates the process of green synthesis of titanium nanoparticles using Erythrina *variegata*. Picture A demonstrates the first step of adding titanium (IV) butoxide to ethanol. Picture B depicts the addition of aqueous *E. variegata* root bark extract. Lastly, picture C illustrates the hardened precipitate after drying in the oven overnight at 65 degrees Celsius.

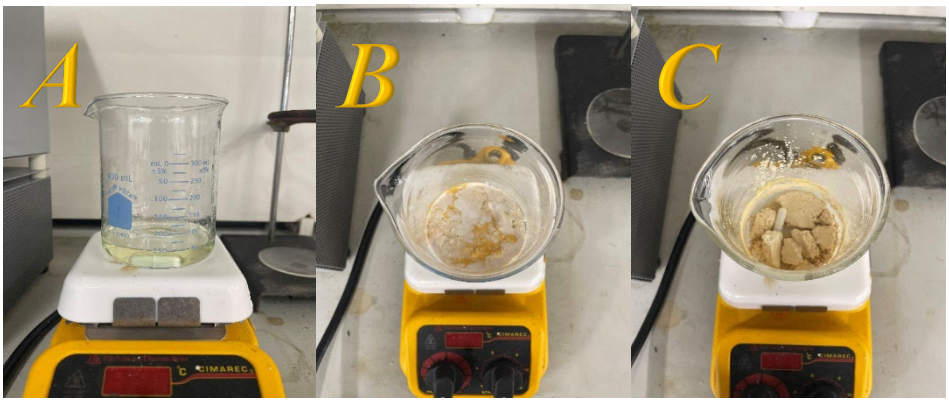

Fig. 16. EvTiNP synthesis procedure: (a) addition of titanium (IV) butoxide to ethanol, (b) addition of aqueous E. *variegata* root bark extract, (c) hardened precipitate after drying.

4.6 UV-Visible Spectroscopy Characterization

Fig. 17 represents the respective UV-visible spectra for *E. variegata*, EvAgNPs, and EvTiNPs. Differences between the EvAgNP and *E. variegata* spectra include increased absorbance of the peaks in the 250-350 nm region and an additional peak at 425 nm. Compared to the *E. variegata* and EvAgNP spectrum, the EvTiNP spectrum completely differs, with only a single peak at 332 nm.

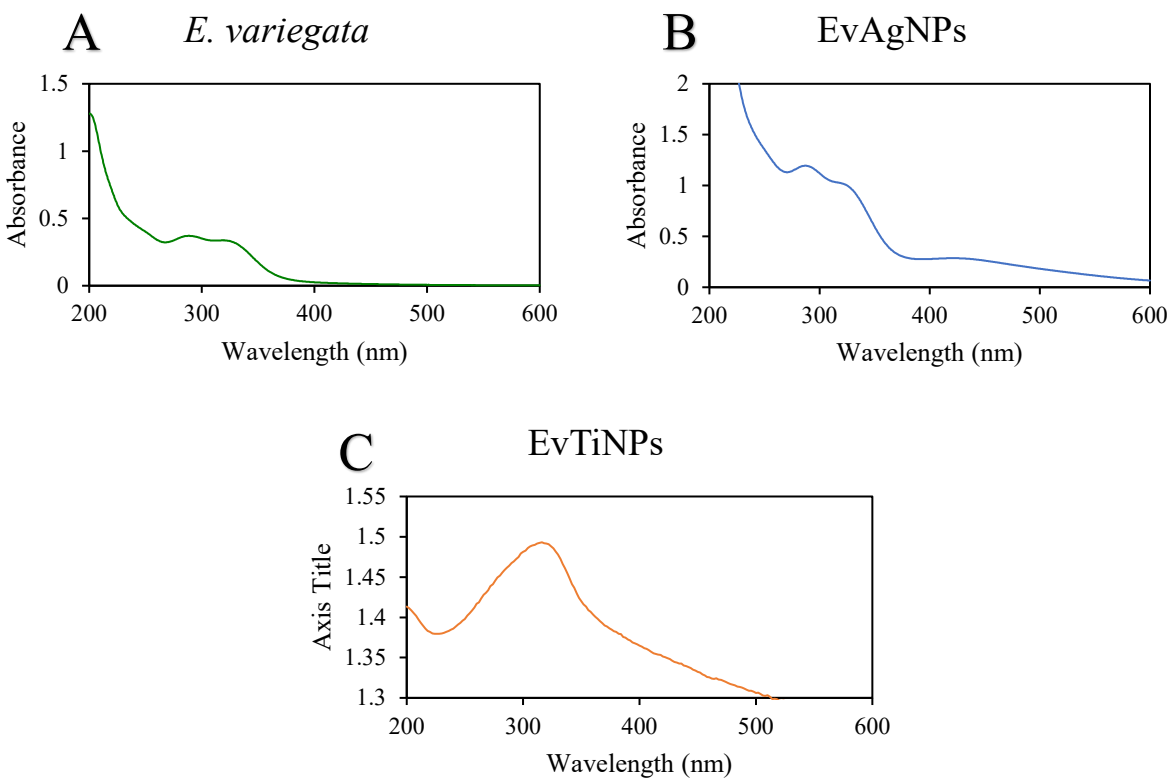

Fig. 17. UV-visible spectra of (a) aqueous E. *variegata* root bark, (b) EvAgNPs, and (c) EvTiNPs.

4.7 Fourier Transform Infrared Spectroscopy

Fig. 18, 19, and 20 represent the FTIR spectra for the *E. variegata* extract, EvAgNPs, and EvTiNPs. The *E. variegata* spectrum shows observable peaks in the range of 3600-3200 cm^{-1}, 2200-2100 cm^{-1}, 1600 cm^{-1}, and 800-400 cm^{-1}. The EvAgNP FTIR spectrum contains the same peaks as the root bark extract spectra but has an additional peak between 2400-2300 cm^{-1}. The EvTiNP spectrum shows a broad peak at 3600 $cm^{-1,}$ a sharp stretching peak between 3200-3000 cm^{-1}, a smaller 1600 cm^{-1} peak, and a strong peak from 800-400 cm^{-1}. Table 9 is an FTIR interpretation chart used to assign the types of chemical bonds and vibrational modes present in a compound.

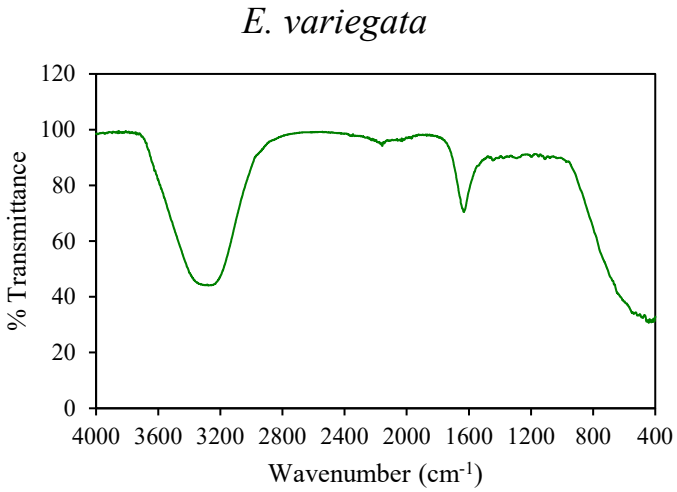

Fig.18. E. *variegata* FTIR spectrum.

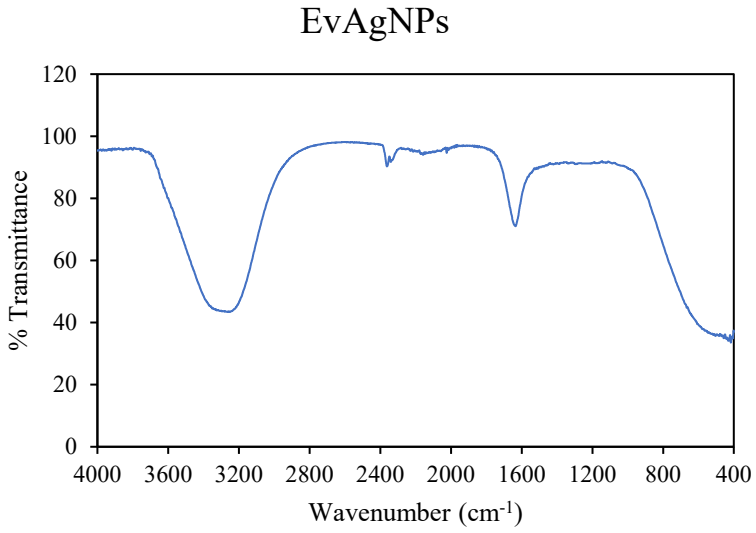

Fig. 19. EvAgNP FTIR spectrum.

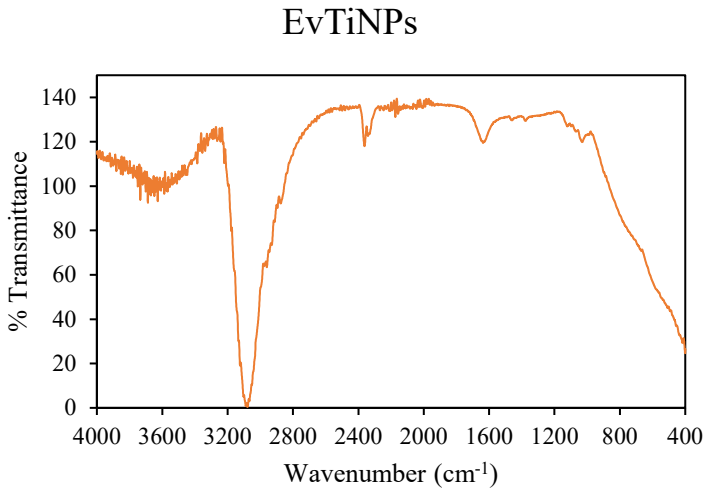

Fig. 20. EvTiNP FTIR spectrum.

TABLE IX

FTIR INTERPRETATION CHART

Type of Vibration			Frequency (cm^{-1})	Intensity
C−H	Alkanes	(stretch)	3000–2850	s
	$-CH_3$	(bend)	1450 and 1375	m
	$-CH_2-$	(bend)	1465	m
	Alkenes	(stretch)	3100–3000	m
		(out-of-plane bend)	1000–650	s
	Aromatics	(stretch)	3150–3050	s
		(out-of-plane bend)	900–690	s
	Alkyne	(stretch)	ca. 3300	s
	Aldehyde		2900–2800	w
			2800–2700	w
C−C	Alkane		Not interpretatively useful	
C=C	Alkene		1680–1600	m–w
	Aromatic		1600 and 1475	m–w
C≡C	Alkyne		2250–2100	m–w
C=O	Aldehyde		1740–1720	s
	Ketone		1725–1705	s
	Carboxylic acid		1725–1700	s
	Ester		1750–1730	s
	Amide		1700–1640	s
	Anhydride		1810 and 1760	s
	Acid chloride		1800	s
C−O	Alcohols, ethers, esters, carboxylic acids, anhydrides		1300–1000	s
O−H	Alcohols, phenols			
	Free		3650–3600	m
	H-bonded		3400–3200	m
	Carboxylic acids		3400–2400	m
N−H	Primary and secondary amines and amides			
	(stretch)		3500–3100	m
	(bend)		1640–1550	m–s
C−N	Amines		1350–1000	m–s
C=N	Imines and oximes		1690–1640	w–s
C≡N	Nitriles		2260–2240	m
X=C=Y	Allenes, ketenes, isocyanates, isothiocyanates		2270–1940	m–s
N=O	Nitro ($R-NO_2$)		1550 and 1350	s
S−H	Mercaptans		2550	w
S=O	Sulfoxides		1050	s
	Sulfones, sulfonyl chlorides, sulfates, sulfonamides		1375–1300 and 1350–1140	s
C−X	Fluoride		1400–1000	s
	Chloride		785–540	s
	Bromide, iodide		< 667	s

4.8 Cyclic Voltammetry

Fig. 21- 26 represent the cyclic voltammograms for *E. variegata*, EvAgNPs, and EvTiNP solutions. Each sample was tested in PBS and tris-HCl buffer. The oxidation-reduction potential was observable for each sample in both solutions, but the voltammogram for *E. variegata* and EvAgNPs in PBS showed greater redox capability. The opposite was true for the EvTiNPs, which exhibited better redox capability in the tris-HCl buffer.

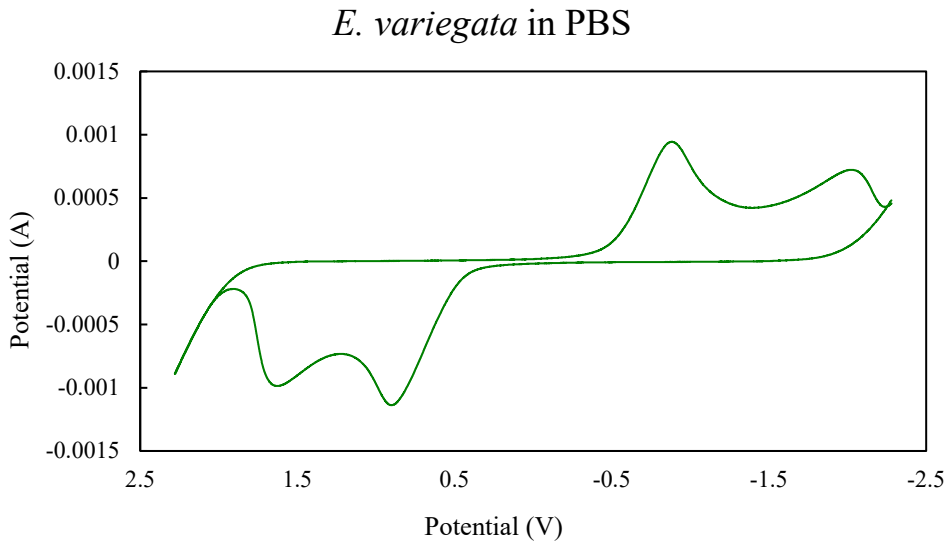

Fig. 21. Cyclic Voltammogram for E. *variegata* in PBS.

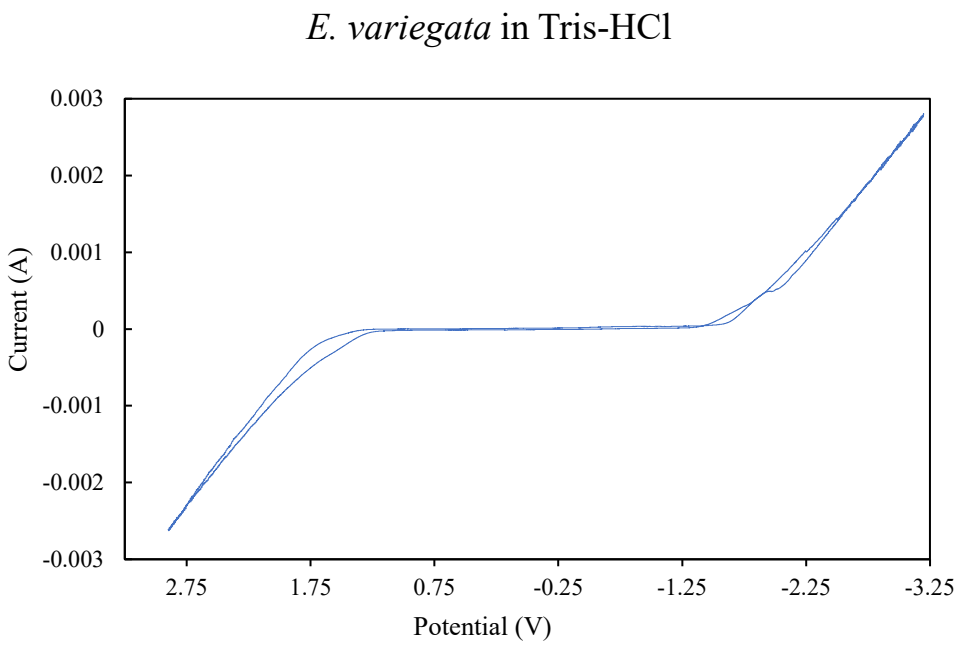

Fig. 22. Cyclic Voltammogram for E. *variegata* in Tris-HCl.

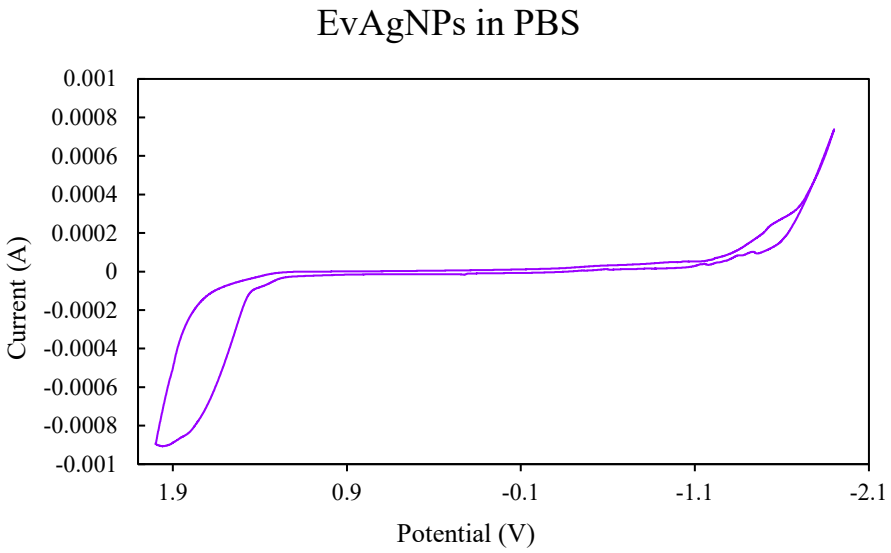

Fig. 23. Cyclic Voltammogram for EvAgNPs in PBS.

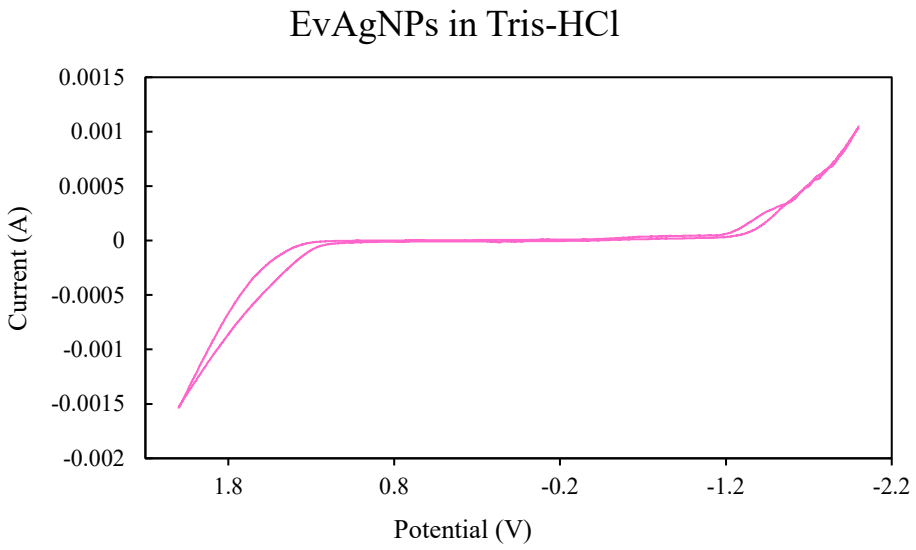

Fig. 24. Cyclic Voltammogram for EvAgNPs in Tris-HCl.

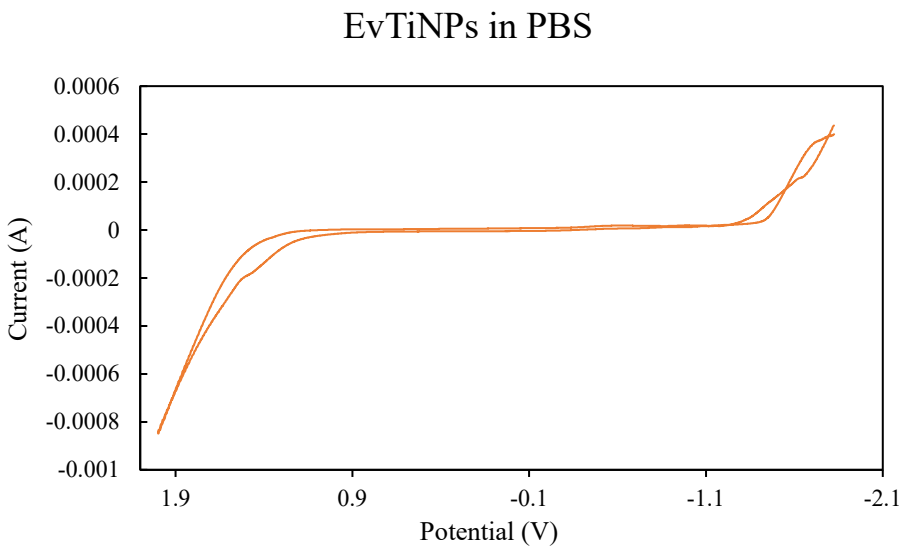

Fig. 25. Cyclic Voltammogram for EvTiNPs in PBS.

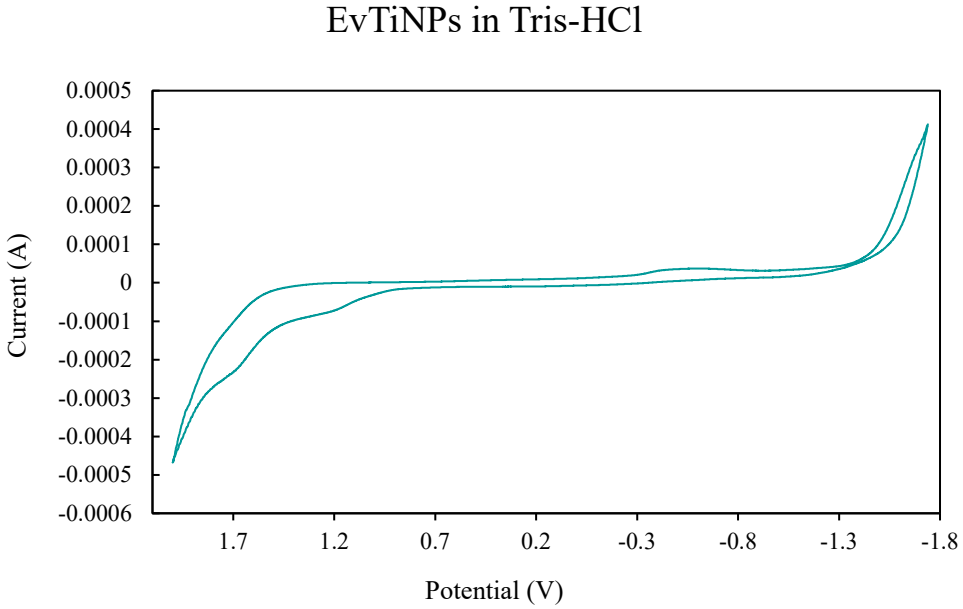

Fig. 26. Cyclic Voltammogram for EvTiNPs in Tris-HCl.

4.9 Scanning Electron Microscopy (SEM)

Fig. 27 and 28 illustrate the backscattered images obtained in the SEM experiments. Fig. 27 presents the SEM images for the EvAgNPs at 200x and 1000x. Fig. 28 shows the SEM image for the EvTiNPs at 3000x.

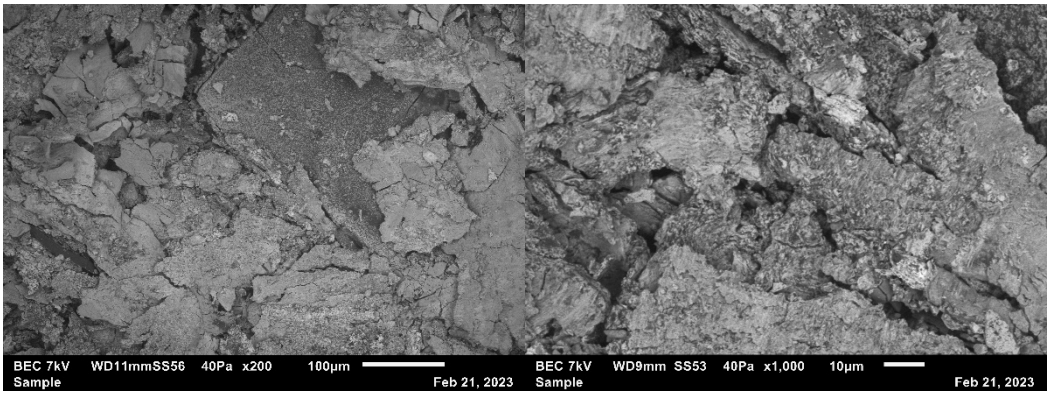

Fig. 27. SEM images for EvAgNPs at 200x (left) and 1000x (right).

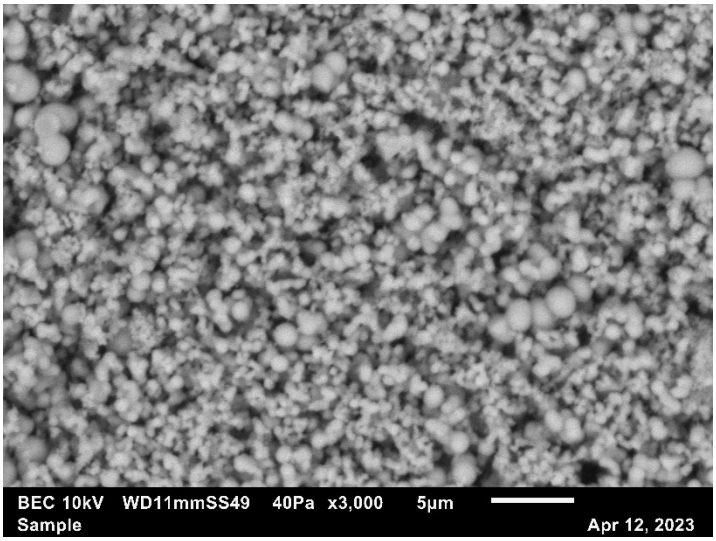

Fig. 28. SEM image for EvTiNP at 3000x.

4.10 Energy Dispersive X-ray Spectroscopy (EDS)

Fig. 29 and Table 10 represent the EvAgNP EDS spectrum and analysis of elements in the EvAgNP sample. Elements identified in the EvAgNP sample include carbon, oxygen, chlorine, and silver. Fig. 30 and Table 11 present the EvTiNP EDS spectrum and the analysis of compounds present in the sample. Elements in the EvTiNP sample consist of carbon, oxygen, and titanium.

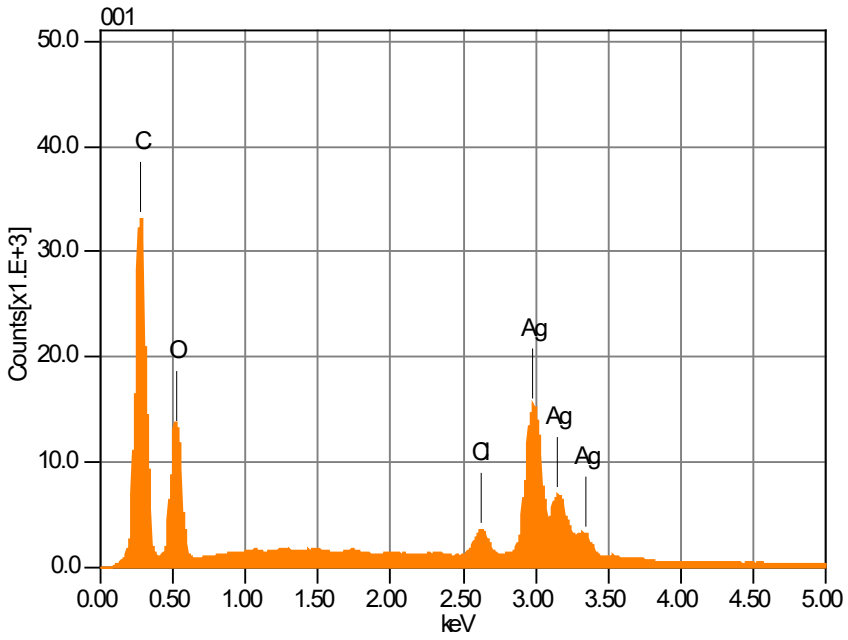

Fig. 29. EvAgNP EDS spectrum.

TABLE X

EDS ANALYSIS OF ELEMENTS PRESENT IN THE EVAGNP SAMPLE

Chemical formula	mass%	Atom%	Sigma	Net	K ratio	Line
C	29.15	59.94	0.01	751774	0.180922	K
O	17.38	26.83	0.03	303291	0.214689	K
Cl	2.12	1.47	0.02	85042	0.102792	K
Ag	51.36	11.76	0.11	984513	1.771558	L
Total	100	100				

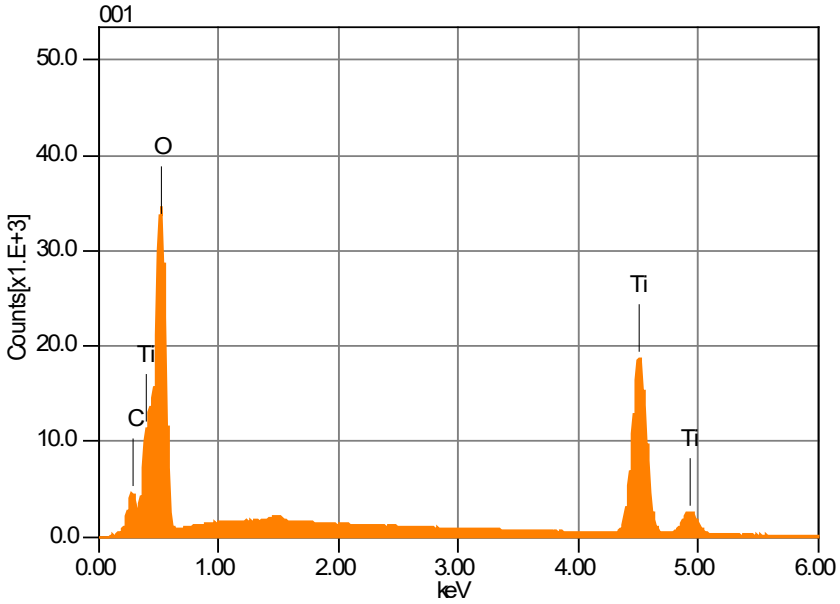

Fig. 30. EvTiNP EDS spectra.

TABLE XI

EDS ANALYSIS OF ELEMENTS PRESENT IN THE EVTINP SAMPLE

Chemical formula	mass%	Atom%	Sigma	Net	K ratio	Line
C	2.41	5.62	0	73422	0.01767	K
O	32.13	56.17	0.04	691726	0.489648	K
Ti	65.46	38.22	0.08	1068278	3.989104	K
Total	100	100				

4.11 Dynamic Light Scattering

Fig. 31 and 32 present the DLS average particle size measurements for the EvAgNP and EvTiNP samples.

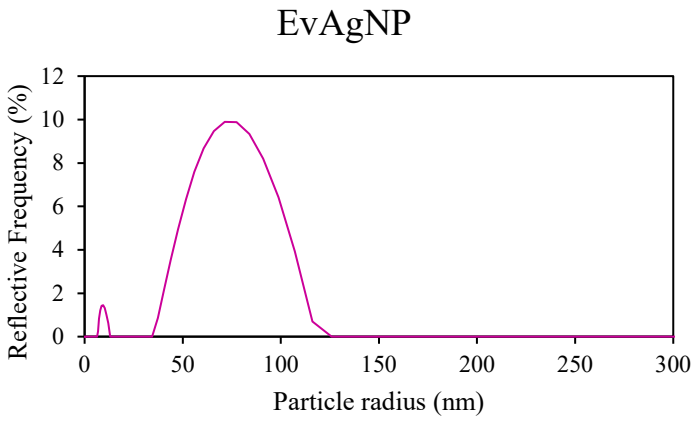

Fig. 31. DLS particle size measurement for EvAgNPs.

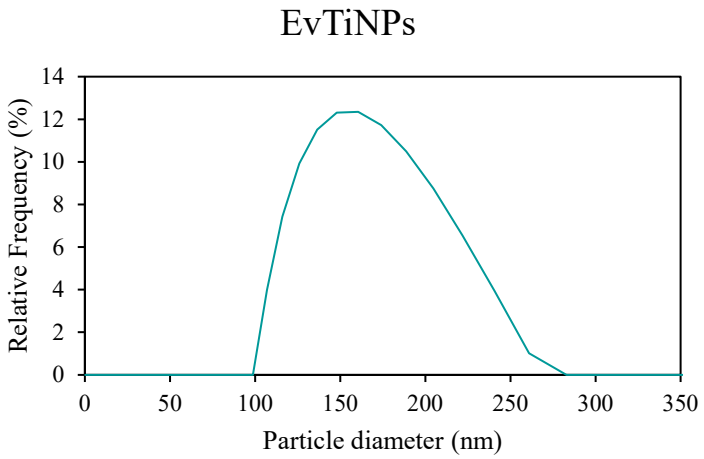

Fig. 32: DLS particle size measurement for EvTiNPs.

4.12 DPPH Assay

Fig. 33 represents the tested samples after adding DPPH and an incubation time of 30 minutes. Scavenging ability can be visually observed by a color change of dark purple to light yellow. Table 12 presents the scavenging ability of the samples tested values are presented ± the standard deviation when n=3. Scavenging abilities were compared to ascorbic acid and E. variegata, and EvAgNP antioxidant activity increased in a concentration-dependent matter. The EvAgNPs were less successful at scavenging the DPPH free radical than E. variegata alone but maintained some of the plant's scavenging ability.

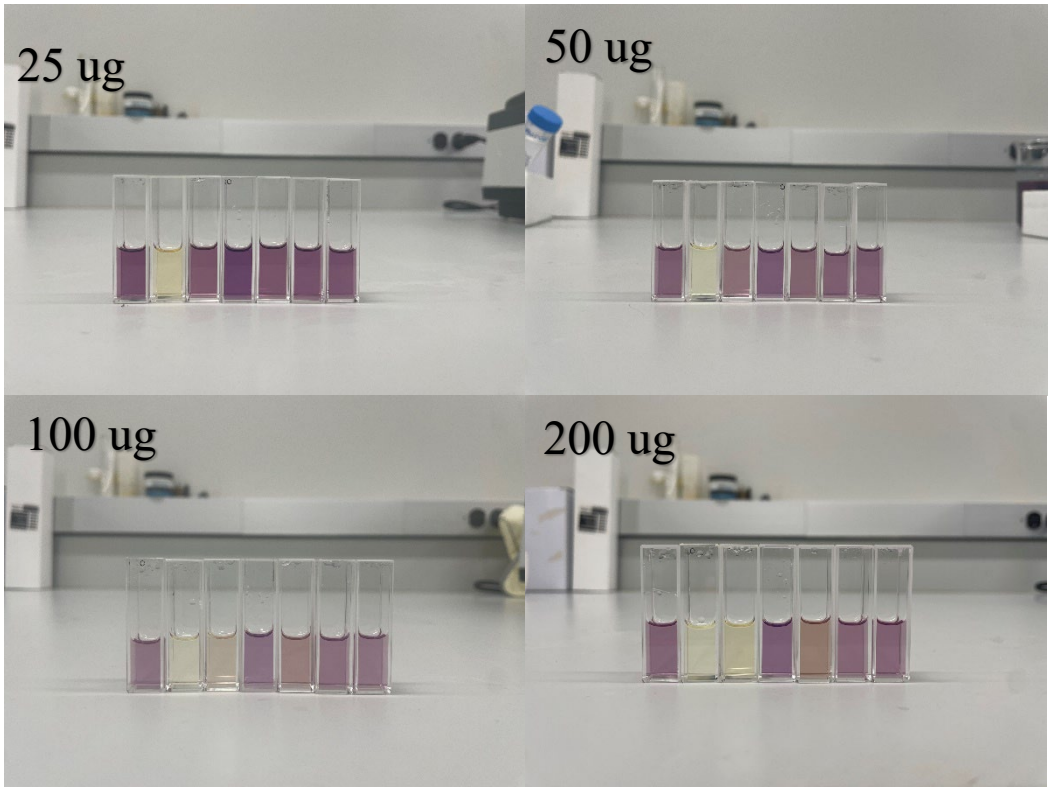

Fig. 33. Samples after adding DPPH (left to right): Control, Ascorbic Acid, *E. variegata*, Silver nitrate control, EvAgNPs, TiO_2 control, EvTiNPs.

TABLE XII

DPPH SCAVENGING ABILITY OF SAMPLES: (a) ASCORBIC ACID, (b) E. *VARIEGATA*, (c) EVAGNPS, AND (d) EVTINPS

Sample No.	**Sample**	**Concentration (ug/mL)**	**DPPH Scavenging ability (%)**
1	Ascorbic Acid	25	94.38 ± 0.04
		50	97.13 ± 0.01
		100	96.34 ± 0.01
		200	97.68 ± 0.01
2	*E. variegata*	25	19.01 ± 0.32
		50	23.78 ± 0.17
		100	44.93 ± 0.22
		200	79.54 ± 0.02
3	EvAgNPs	25	10.61 ± 0.29
		50	7.39 ± 0.16
		100	13.94 ± 0.23
		200	26.56 ± 0.05
4	EvTiNPs	25	3.39 ± 0.30
		50	1.07 ± 0.17
		100	0.00 ± 0.25
		200	0.76 ± 0.08

4.13 Nitric Oxide Assay

Fig. 34 and Table 13 present the nitric oxide scavenging assay results. Fig. 14 shows the tested samples following a two-hour incubation time and the addition of the Griess reagent. Samples effective in scavenging the nitric oxide free radical will have an observably lighter color due to the sample's ability to degrade the colored azo product formed after the Griess reagent addition. Table 13 shows the scavenging ability values for each tested sample. Compared to the ascorbic acid sample, *E. variegata,* EvAgNPs, and EvTiNPs showed marked antioxidant effectiveness against the nitric oxide free radical. The EvAgNP and EvTiNP solutions were also able to enhance the plant's natural nitric oxide scavenging ability.

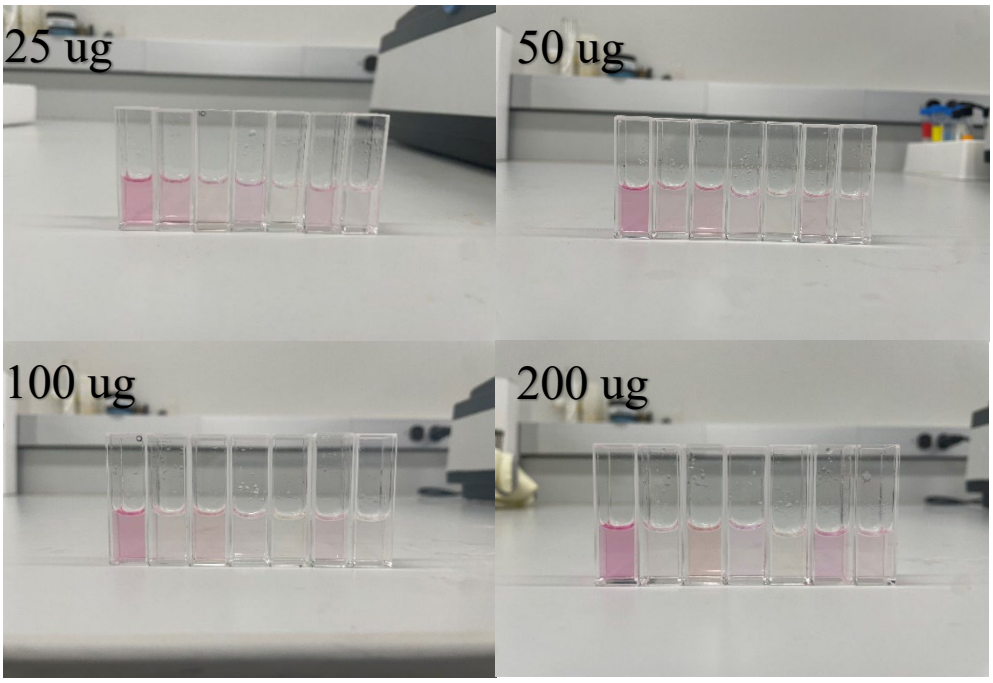

Fig. 34. Samples after adding Sodium Nitroprusside (left to right): Control, Ascorbic Acid, E. *variegata*, silver nitrate control, EvAgNPs, TiO_2 control, EvTiNPs.

TABLE XIII

SCAVENGING ABILITY OF SAMPLES: (a) ASCORBIC ACID, (b) E. *VARIEGATA*, (c) EVAGNPS, AND (d) EVTINPS

Sample No.	Sample	Concentration (ug/mL)	NO Scavenging ability (%)
1	Ascorbic Acid	25	43.96 ± 0.02
		50	42.70 ± 0.02
		100	64.90 ± 0.03
		200	71.25 ± 0.04
2	*E. variegata*	25	67.59 ± 0.02
		50	61.29 ± 0.02
		100	58.68 ± 0.01
		200	55.43 ± 0.03
3	EvAgNPs	25	85.88 ± 0.02
		50	86.47 ± 0.02
		100	87.39 ± 0.01
		200	81.89 ± 0.01
4	EvTiNPs	25	66.59 ± 0.03
		50	77.41 ± 0.01
		100	70.46 ± 0.01
		200	69.77 ± 0.01

4.14 MTS Assay

Fig. 35 presents the data obtained in the MTS assay for *E. variegata*, the TiO_2 control, and the EvTiNP solutions. Values show a marked decrease in H358 cell line viability, with the *E. variegata* root bark extract alone showing the most significant effectiveness.

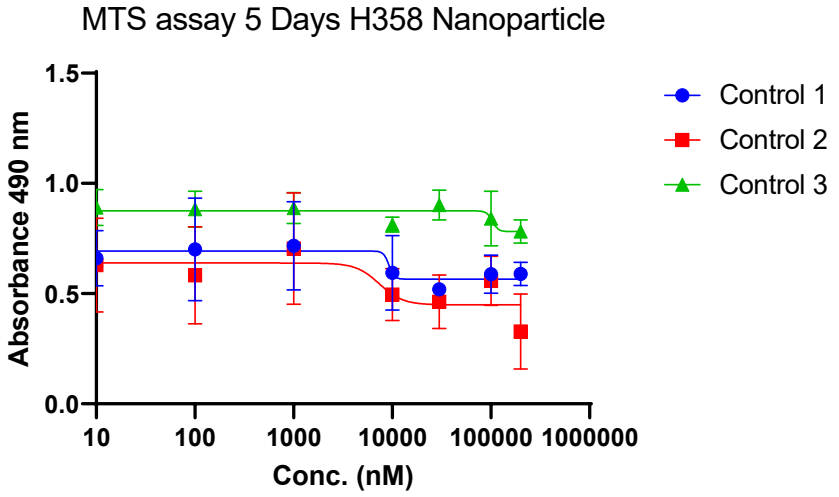

	Control 1			Control 2			Control 3		
X	A:Y1	A:Y2	A:Y3	B:Y1	B:Y2	B:Y3	C:Y1	C:Y2	C:Y3
200000	0.5581	0.5592	0.6496	0.4399	0.4134	0.1317	0.7276	0.7848	0.8322
100000	0.5057	0.5816	0.6780	0.6844	0.5183	0.4706	0.6973	0.9018	0.9214
30000	0.4922	0.5196	0.5479	0.5981	0.4272	0.3627	0.8839	0.9766	0.8449
10000	0.7876	0.5201	0.4736	0.6179	0.4867	0.3834	0.7978	0.8514	0.7891
1000	0.8849	0.7716	0.4959	0.9782	0.6551	0.4784	0.8066	0.9308	0.9282
100	0.8246	0.8445	0.4315	0.8374	0.4625	0.4492	0.9293	0.9326	0.7892
10	0.7690	0.6921	0.5225	0.8730	0.5322	0.4831	0.9520	0.7977	0.9236
0	0.9036	0.8387	0.4670	0.7089	0.7457	0.8804	0.9963	0.8206	0.9363

Fig. 35. MTS Assay absorbance readings at 490 nm for samples: Control 1: TiO_2, Control 2: E. *variegata*, and Control 3: EvTiNPs.

5. DISCUSSION AND CONCLUSION

5.1 Discussion

The plant used for the work in this thesis was confirmed to be *Erythrina variegata.* Analysis of the gas chromatogram and mass spectra for the methanolic root bark extract of *E. variegata* confirmed that the sample was from the *Erythrina* species due to the presence of 3-eicosyne, 3, 7, 11, 15-tetramethyl-2-hexadecen-1-ol, phytol, 2-hexadecen-1-ol, 3,7,11, 15-tetramethyl-, 1,2-benzenedicarboxylic acid, diundecyl ester, and 1-octanol, 2-butyl. The observed phytochemical profile of the methanolic root bark extract aligned with the current literature on *E. variegata* and the compounds present attested to the plant's success in the antioxidant and cytotoxic assessments of this thesis. The characterization studies revealed the successful formation of silver and titanium nanoparticles using aqueous *E. variegata* root bark extract. The UV-visible spectra confirmed the formation of silver and titanium nanoparticles using the *E. variegata* root bark extract. Compared to the absorbance spectrum of the aqueous root bark alone, the absorption peak between 400-500 nm confirms the presence of AgNPs, and the absorption peak between 275-500 nm confirms the presence of TiNPs. The FTIR spectra for the root bark extract, EvAgNPs, and EvTiNPs each contain observable differences. The spectra for the root bark extract, EvAgNPs, and EvTiNPs each contained visible differences. The *E. variegata* root bark extract spectrum had peaks in the range of 3600-3200 cm^{-1}, 2200-2100 cm^{-1}, 1600 cm^{-1}, and 800-400 cm^{-1}. These peaks indicated the presence of an O-H bond, an aromatic ring, a C-C alkene bond, and an alkyl halide, respectively. The EvAgNP FTIR spectrum contained the same peaks as the root bark

extract spectra but had an additional peak between 2400-2300 cm^{-1}. This additional peak likely indicated the presence of an alkyne group. The resulting EvTiNP FTIR spectrum notably differed from the root bark extract and EvAgNP spectra. There was a broad peak at 3600 $cm^{-1,}$ indicating the presence of a free O-H group, a sharp aromatic stretching peak between 3200-3000 cm^{-1}, a smaller 1600 cm^{-1} peak, and a stronger peak from 800-400 cm^{-1}. The 2400-2300 cm-1 peak also shifted closer to 2400 cm^{-1}. The electrochemical studies revealed significant oxidation and reduction potential. The *E. variegata* root bark extract and the EvAgNPs showed greater redox capabilities in PBS, while the EvTiNPs showed stronger redox potential in the tris-HCl buffer. The EDS elemental analysis demonstrated that the EvAgNP and EvTiNP samples were largely composed of silver and titanium, respectively. The Dynamic Light Scattering experiments showed that the EvAgNP's particle size falls within the accepted size of nanomaterials for biological applications at a measured size of 81.62 nm. The EvTiNPs fell slightly outside the accepted range for biological applications at a measured size of 218.04 nm. The larger size of the EvTiNPs was likely attributed to the aggregation of the nanoparticles, which is a known issue in nanoparticle experimentation.

For the DPPH antioxidant assay, *E. variegata* showed a marked scavenging ability of the free radical. The silver and titanium nanoparticles were unable to enhance the plant's natural antioxidant capabilities, but the EvAgNPs were able to maintain some of the antioxidant properties. The EvTiNPs did not exhibit any scavenging efficiency in inhibiting the generation of the DPPH free radical. The limited functionality of the EvTiNPs in this assay could result from larger particle size, but additional studies would need to be done to confirm this. The EvAgNP and EvTiNP results for the nitric oxide

scavenging assay were considerably better than those of the DPPH assay. The EvAgNPs and EvTiNPs achieved a higher scavenging percentage in the nitric oxide assay than *E. variegata,* demonstrating that both nanoparticle samples could enhance the plant's ability to inhibit the nitric oxide free radical formation. The MTS assay showed marked effectiveness in reducing the cell viability of the H358 cells, confirming the known anticancer properties of *E. variegata* and providing additional insight into titanium's ability to maintain those properties.

5.2 Conclusion

This thesis successfully characterized silver and titanium nanoparticles synthesized using *Erythrina variegata* root bark, documenting another avenue for green synthesis of nanoparticles. Through characterization, the work performed in this study expanded the current knowledge and literature regarding the plant and its potential for nanoparticle synthesis and applications. The results of this study indicate there is potential to use nanoparticles synthesized with *E. variegata.* Future studies should examine the extent these natural products can have in anticancer treatment, drug delivery, and addressing issues caused by reactive oxygen and nitrogen species in the environment and the human body.

REFERENCES

1. A. G. Atanasov et al., “Discovery and Resupply of Pharmacologically Active Plant-Derived Natural Products: A Review,” Biotechnology Advances, vol. 33, no. 8, pp. 1582-1614, 2015.

2. N. E. Thomford et al., “Pharmacogenomics Implications of Using Herbal Medicinal Plants on African Populations in Health Transition,” Pharmaceuticals, vol. 8, no. 3, pp. 637-663, 2015.

3. A. S. Van Wyk and G. Prinsloo, “Health, Safety and Quality Concerns of Plant-Based Traditional Medicines and Herbal Remedies,” South African Journal of Botany, vol. 133, pp. 54-62, 2020.

4. B. David, J.-L. Wolfender, and D. A. Dias, “The Pharmaceutical Industry and Natural Products: Historical Status and New Trends,” Phytochemistry Reviews, vol. 14, no. 2, pp. 299-315, 2015.

5. R. El-Tanbouly, Z. Hassan, and S. El-Messeiry, “The Role of Indoor Plants in Air Purification and Human Health in the Context of COVID-19 Pandemic: A Proposal for a Novel Line of Inquiry,” Frontiers in Molecular Biosciences, vol. 8, 709395, 2021.

6. R. N. Bharagava, G. Saxena, and S. I. Mulla, “Introduction to Industrial Wastes Containing Organic and Inorganic Pollutants and Bioremediation Approaches for Environmental Management,” in Bioremediation of Industrial Waste for Environmental Safety, G. Saxena and R. N. Bharagava, Eds. Singapore: Springer, 2020, pp. 1-18.

7. R. Cassia et al., “Climate Change and the Impact of Greenhouse Gasses: CO2 and NO, Friends and Foes of Plant Oxidative Stress,” Frontiers in Plant Science, vol. 9, 273, 2018.

8. G. D. Thurston, “Outdoor Air Pollution: Sources, Atmospheric Transport, and Human Health Effects.”

9. S. Lingadurai, A. Jain, N. Barman, and A. Kumar, “Erythrina Variegata Linn: A Review on Morphology, Phytochemistry, and Pharmacological Aspects,” Pharmacognosy Reviews, vol. 4, no. 8, pp. 147-152, 2010.

10. I. Papanicolas and L. Woskie, “Chapter 4: The Current State of Global Health Care Quality,” 2018, pp. 129-167.

11. T. K. Lim, Edible Medicinal And Non-Medicinal Plants: Volume 7, Flowers, 2014, pp. 788-806.

12. A. Kumar, S. Lingadurai, A. Jain, and N. R. Barman, “Erythrina variegata Linn: A review on morphology, phytochemistry, and pharmacological aspects,” Pharmacognosy Reviews, vol. 4, no. 8, pp. 147–152, 2010. Available:

13. “The Wealth of India: A Dictionary of Indian Raw Materials and Industrial Products (Industrial Products—Part I),” The Indian Medical Gazette, vol. 84, no. 10, pp. 476-477, 1949.

14. M. Z. Rahman, M. Rahman, A. Kaisar, A. Hossain, and M. Rashid, “Bioactive Isoflavones from Erythrina Variegata L.,” Turkish Journal of Pharmaceutical Sciences, vol. 7, pp. 21-28, 2010.

15. W. Y. Ahmad, I. K. Said, S. Y. Soon, H. Takayama, M. Kitajima, and N. Aimi, "A pterocarpan from Erythrina variegata," Journal of Biological Sciences, vol. 2, pp. 542-544, 2002.

16. S. Muthukrishnan, S. Palanisamy, S. Subramanian, S. Selvaraj, K. R. Mari, and R. Kuppulingam, “Phytochemical Profile of Erythrina Variegata by Using High-Performance Liquid Chromatography and Gas Chromatography-Mass Spectroscopy Analyses,” Journal of Acupuncture and Meridian Studies, vol. 9, no. 4, pp. 207-212, 2016.

17. “Metabocard for 3-Eicosyne,”

18. “Dr.Duke’s Phytochemical and Ethnobotanical Databases,”

19. R. Neelamegam and B. Ezhilan, “GC-MS Analysis of Phytocomponents in the Ethanol Extract of Polygonum Chinense L.,” Pharmacognosy Research, vol. 4, no. 1, pp. 11-14, 2012.

20. M. Sermakkani and V. Thangapandian, “GC-MS Analysis of Cassia Italica Leaf Methanol Extract,” Asian Journal of Pharmaceutical and Clinical Research, vol. 5, pp. 90-94, 2012.

21. B. Venkata Raman et al., “Antibacterial, Antioxidant Activity and GC-MS Analysis of Eupatorium Odoratum,” Asian Journal of Pharmaceutical and Clinical Research, vol. 5, 2012.

22. T. R. Sudha, S. Chidambarampillai, and V. R. Mohan, “GC-MS ANALYSIS OF BIOACTIVE COMPONENTS OF AERIAL PARTS OF KIRGANELIA RETICULATA POIR (EUPHORBIACEAE),” 2013.

23. R. S. Amarowicz, “Squalene: A Natural Antioxidant?” European Journal of Lipid Science and Technology, vol. 111, pp. 411-412, 2009.

24. C. Rao, H. Newmark, and B. Reddy, “Chemopreventive Effect of Squalene on Colon Cancer,” Carcinogenesis, vol. 19, pp. 287-290, 1998.

25. S. Sunitha, N. Manickam, and P. Varalakshmi, “Hepatoprotective Effect of Lupeol and Lupeol Linoleate on Tissue Antioxidant Defence System in Cadmium-Induced Hepatotoxicity in Rats,” Fitoterapia, vol. 72, pp. 516-523, 2001.

26. M. Ukiya et al., "Constituents of Compositae Plants III. Anti-Tumor Promoting Effects and Cytotoxic Activity against Human Cancer Cell Lines of Triterpene Diols and Triols from Edible Chrysanthemum Flowers,” Cancer Letters, vol. 177, pp. 7-12, 2002.

27. D. Katerere, A. Gray, R. Nash, and R. Waigh, “Antimicrobial Activity of Pentacyclic Triterpenes Isolated from African Combretaceae,” Phytochemistry, vol. 63, pp. 81-88, 2003.

28. M. Inoue et al., “Role of Reactive Oxygen Species in Gallic Acid-Induced Apoptosis,” Biological & Pharmaceutical Bulletin, vol. 23, pp. 1153-1157, 2000.

29. M. S. Y. et al., “Antioxidant and Antimicrobial Properties of Phenolic Rich Fraction of Seabuckthorn (Hippophae Rhamnoides L.) Leaves in Vitro,” Food Chemistry, vol. 141, pp. 3443-3450, 2013.

30. C.-H. Peng et al., “Mulberry Water Extracts Possess an Anti-Obesity Effect and Ability to Inhibit Hepatic Lipogenesis and Promote Lipolysis,” Journal of Agricultural and Food Chemistry, vol. 59, no. 6, pp. 2663-2671, 2011. Available:

31. S.-H. Wang et al., “Oral Administration of Trapa Taiwanensis Nakai Fruit Skin Extracts Conferring Hepatoprotection from CCl4-Caused Injury,” Journal of Agricultural and Food Chemistry, vol. 59, pp. 3686-3692, 2011. Available:

32. Z. Lu et al., “Structure–Activity Relationship Analysis of Antioxidant Ability and Neuroprotective Effect of Gallic Acid Derivatives,” Neurochemistry International, vol. 48, pp. 263-274, 2006.

33. C.-Y. Hsiang et al., “Toona Sinensis and Its Major Bioactive Compound Gallic Acid Inhibit LPS-Induced Inflammation in Nuclear Factor-κB Transgenic Mice as Evaluated by in Vivo Bioluminescence Imaging,” Food Chemistry, vol. 136, pp. 426-434, 2013.

34. B. H. Kroes et al., “Anti-Inflammatory Activity of Gallic Acid,” Planta Medica, vol. 58, pp. 499-504, 1992.

35. B. H. Kroes et al., “Anti-Inflammatory Activity of Gallic Acid,” Planta Medica, vol. 58, pp. 499-504, 1992.

36. C.-L. Hsu and G.-C. Yen, “Effect of Gallic Acid on High Fat Diet-Induced Dyslipidaemia, Hepatosteatosis and Oxidative Stress in Rats,” The British Journal of Nutrition, vol. 98, pp. 727-735, 2007.

37. A. Jang et al., “Comparison of Hypolipidemic Activity of Synthetic Gallic Acid–Linoleic Acid Ester with Mixture of Gallic Acid and Linoleic Acid, Gallic Acid, and Linoleic Acid on High-Fat Diet Induced Obesity in C57BL/6 Cr Slc Mice,” Chemico-Biological Interactions, vol. 174, no. 2, pp. 109-117, 2008. Available:

38. H. O. Saxena et al., “Gallic Acid-Based Indanone Derivatives as Anti-cancer Agents,” Bioorganic & Medicinal Chemistry Letters, vol. 18, no. 14, pp. 3914-3918, 2008.

39. M. Esteves et al., “Antioxidant Versus Cytotoxic Properties of Hydroxycinnamic Acid Derivatives – A New Paradigm in Phenolic Research,” Archiv der Pharmazie, vol. 341, pp. 164-173, 2008.

40. M. Inoue et al., “Antioxidant, Gallic Acid, Induces Apoptosis in HL-60RG Cells,” Biochemical and Biophysical Research Communications, vol. 204, no. 2, pp. 898-904, 1994.

41. H.-M. Chen et al., “Gallic Acid, a Major Component of Toona Sinensis Leaf Extracts, Contains a ROS-Mediated Anti-Cancer Activity in Human Prostate Cancer Cells,” Cancer Letters, vol. 286, no. 2, pp. 161-171, 2009.

42. J. Martins and B. Sukumaran, “Anti-Depressant Activity of Erythrina Variegata Bark Extract and Regulation of Monoamine Oxidase Activities in Mice,” Journal of Ethnopharmacology, vol. 248, 112280, 2019.

43. G. U. Nethaji S., “Determination of bioactive compounds from Erythrina variegata leaf extract using gas chromatographic and mass spectroscopic techniques,” International Journal of Botany Studies, vol. 6, no. 2, pp. 111-114, 2021.

44. C. Crevost and A. Petelot, "Catalogue des produits de L’Indochine. Plantes Med," Bull Econ Indochine. Impr. d’Extrême-Orient, 322 pp, 1928.

45. I. H. Burkill, “A dictionary of the economic products of the Malay Peninsula,” Revised reprint, Ministry of Agriculture and Co-operatives, Kuala Lumpur, Malaysia, vol. 1 (A–H), pp. 1–1240, vol. 2 (I–Z), pp. 1241–2444, 1966.

46. World Health Organisation (WHO), “Medicinal plants in the South Pacific,” WHO Regional Publications Western Pacific series no 19, 151 pp, 1998.

47. G. U. Stuart, “Philippine alternative medicine,” Manual of some Philippine medicinal plants, 2012.

48. S. Sakat and A. Juvekar, “Comparative Study of Erythrina Indica Lam. (Fabaceae) Leaves Extracts for Antioxidant Activity,” Journal of Young Pharmacists, vol. 2, 2010.

49. R. John, J. K. Bibu, and P. T. A. Usha, “In Vitro Antioxidant Activity of Methanol Extract of Erythrina Variegata Stem Bark,” Int. J. Appl. Pure Sci. Agric., vol. 4, no. 3, pp. 18-22, 2018.

50. L. Xiaoli et al., “Four New Isoflavonoids from the Stem Bark of Erythrina Variegata,” Chemical and Pharmaceutical Bulletin, vol. 54, no. 4, pp. 570-573, 2006.

51. H. Ohba et al., “Cytotoxicity Induced by Erythrina Variegata Serine Proteinase Inhibitors in Tumor Hematopoietic Stem Cell Lines,” Bioscience, Biotechnology, and Biochemistry, vol. 62, no. 6, pp. 1166-1170, 1998.

52. T. Herlina et al., “Antimalarial Compound from the Stem Bark of Erythrina Variegata,” Indonesia. J. Chem., vol. 9, 2010.

53. M. Z. Rahman et al., “Phytochemical and Biological Investigations of Erythrina Variegata,” Saudi Pharmaceutical Journal, vol. 15, 2007.

54. H. Zhang et al., “Anti-Tumor Activity of Erythrina Variegata L. Extract and Its Mechanism of Action,” Yao xue xue bao Acta pharmaceutica Sinica, vol. 44, pp. 1359-1363, 2009.

55. T. Herlina et al., “In Vitro Anticancer and Antimalarial Erystagallin-A from Erythrina Variegata (L.) Stem Bark,” Medicinal Plants - International Journal of Phytomedicines and Related Industries, vol. 3, 9, 2011.

56. A. Rasul et al., “Xanthoxyletin, a Coumarin Induces S Phase Arrest and Apoptosis in Human Gastric Adenocarcinoma SGC-7901 Cells,” Asian Pacific Journal of Cancer Prevention : APJCP, vol. 12, pp. 1219–1223, 2011.

57. N. Baskar, B. Devi, and M. Ramar, “Anti-Cancer Activity of Methanol Extract of Root Bark of Erythrina Variegata Linn,” International Journal of Toxicological and Pharmacological Research, vol. 2, pp. 74, 2010.

58. S. Ylä-Herttuala, “Oxidized LDL and Atherogenesis,” Annals of the New York Academy of Sciences, vol. 874, pp. 134–137, 1999.

59. E. R. Stadtman and R. L. Levine, “Protein oxidation,” Annals of the New York Academy of Sciences, vol. 899, pp. 191–208, 2000.

60. L. O. Marnett, “Oxyradicals and DNA Damage,” Carcinogenesis, vol. 21, pp. 361–370, 2000.

61. A. Phaniendra, D. B. Jestadi, and L. Periyasamy, “Free radicals: properties, sources, targets, and their implication in various diseases,” Indian Journal of Clinical Biochemistry: IJCB, vol. 30, no. 1, pp. 11–26, 2015.

62. S. Shiva Samhitha et al., “Green Synthesized TiO2 Nanoparticles for Anticancer Applications: Mini Review,” Materials Today: Proceedings, vol. 54, pp. 765–770, 2022.

63. K. Parveen, V. Banse, and L. Ledwani, “Green Synthesis of Nanoparticles: Their Advantages and Disadvantages,” AIP Conference Proceedings, vol. 1724, 2016.

64. P. Khadka et al., “Pharmaceutical particle technologies: An approach to improve drug solubility, dissolution and bioavailability,” Asian Journal of Pharmaceutical Sciences, vol. 9, pp. 304–316, 2014.

65. S. Barua and S. Mitragotri, “Challenges associated with Penetration of Nanoparticles across Cell and Tissue Barriers: A Review of Current Status and Future Prospects,” Nano Today, vol. 9, pp. 223–243, 2014.

66. P. P. Fu et al., “Mechanisms of nanotoxicity: Generation of reactive oxygen species,” Journal of Food and Drug Analysis, vol. 22, pp. 64–75, 2014.

67. S. Shukla et al., “The Impact of Aspect Ratio on the Biodistribution and Tumor Homing of Rigid Soft-Matter Nanorods,” Advanced Healthcare Materials, vol. 4, pp. 874–882, 2015.

68. A. Tanik et al., “Advances in Water Quality Control,” 2010.

69. W. Zhang, “Nanotechnology for water purification and waste treatment,” in Frontiers in Nanotechnology, Washington, DC: U.S. EPA Millennium Lecture Series, 2005.

70. J. Theron, J. A. Walker, and T. E. Cloete, “Nanotechnology and Water Treatment: Applications and Emerging Opportunities,” Nanotechnology in Water Treatment Applications, pp. 43–69, 2010.

71. C. Kunze et al., “Environmental remediation of radioactively contaminated sites,” Environmental Radiation Survey and Site Execution Manual (EURSSEM), 2010.

72. I. S. Yunus et al., “Nanotechnologies in Water and Air Pollution Treatment,” Environmental Technology Reviews, vol. 1, no. 1, pp. 136–148, 2012.

73. D. L. Jacob et al., “UPTAKE AND TRANSLOCATION OF TI FROM NANOPARTICLES IN CROPS AND WETLAND PLANTS,” International Journal of Phytoremediation, vol. 15, no. 2, pp. 142–153, 2013.

74. N. Elgrishi et al., “A Practical Beginner’s Guide to Cyclic Voltammetry,” Journal of Chemical Education, vol. 95, no. 2, pp. 197–206, 2018.

75. A. J. Bard, R. Parsons, and J. Jordan, eds., “Standard Potentials in Aqueous Solutions,” New York: Dekker, 1985; G. Milazzo, S. Caroli, and V. K. Sharma,

"Tables of Standard Electrode Potentials," Wiley: London, 1978; E. H. Swift and E. A. Butler, "Quantitative Measurements and Chemical Equilibria," Freeman: New York, 1972.

76. V. K. et al., "Green Inspired Synthesis of ZnO Nanoparticles and Its Characterizations with Biofilm, Antioxidant, Anti-Inflammatory, and Anti-Diabetic Activities," Journal of Molecular Structure, vol. 1255, 132420, 2022.

77. M. S. Blois, "Antioxidant Determinations by the Use of a Stable Free Radical," Nature, vol. 181, no. 4617, pp. 1199–1200, 1958.

78. L. C. Green et al., "Analysis of Nitrate, Nitrite, and [15N] Nitrate in Biological Fluids," Analytical Biochemistry, vol. 126, no. 1, pp. 131–138, 1982. Available:

79. V. Kuete and O. Karaosmanoğlu, "Anticancer Activities of African Medicinal Spices and Vegetables," in Medicinal Spices and Vegetables from Africa: Therapeutic Potential Against Metabolic, Inflammatory, Infectious and Systemic Diseases, 2017, pp. 271–297.

80. T. M. Buttke, J. A. McCubrey, and T. C. Owen, "Use of an Aqueous Soluble Tetrazolium/Formazan Assay to Measure Viability and Proliferation of Lymphokine-Dependent Cell Lines," Journal of Immunological Methods, vol. 157, no. 1, pp. 233–240, 1993.

81. A. Cory et al., "Use of an Aqueous Soluble Tetrazolium/Formazan Assay for Cell Growth Assays in Culture," Cancer Communications, vol. 3, no. 7, pp. 207–212, 1991.

82. V. N. Anjana et al., "Microwave Assisted Green Synthesis of Silver Nanoparticles for Optical, Catalytic, Biological and Electrochemical Applications," Artificial Cells, Nanomedicine, and Biotechnology, vol. 49, no. 1, pp. 438–449, 2021.

83. A. Van Tonder, A. M. Joubert, and A. D. Cromarty, "Limitations of the 3-(4,5-Dimethylthiazol-2-Yl)-2,5-Diphenyl-2H-Tetrazolium Bromide (MTT) Assay When Compared to Three Commonly Used Cell Enumeration Assays," BMC Research Notes, vol. 8, 2015.

84. O. Ouerghi et al., "Limon-Citrus Extract as a Capping/Reducing Agent for the Synthesis of Titanium Dioxide Nanoparticles: Characterization and Antibacterial Activity," Green Chemistry Letters and Reviews, vol. 15, no. 3, pp. 483–490, 2022.

85. D. L. Pavia, G. M. Lampman, G. S. Kriz, and J. R. Vyvyan, Introduction to Spectroscopy, 2015.